51
4-3-89 JT (2)

DR# 0767-6

FOSSIL ENERGY

NIPER-392
(DE89000737)

THE EFFECTS OF VISCOUS FORCES ON THREE-PHASE RELATIVE PERMEABILITY

Topical Report

By
D.R. Maloney
S.M. Mahmood
M.M. Honarpour

April 1989

Performed Under Cooperative Agreement No. FC22-83FE60149

IIT Research Institute
National Institute for Petroleum and Energy Research
Bartlesville, Oklahoma

Bartlesville Project Office
U. S. DEPARTMENT OF ENERGY
Bartlesville, Oklahoma

DISTRIBUTION OF THIS DOCUMENT IS UNLIMITED

DISCLAIMER

This report was prepared as an account of work sponsored by an agency of the United States Government. Neither the United States Government nor any agency Thereof, nor any of their employees, makes any warranty, express or implied, or assumes any legal liability or responsibility for the accuracy, completeness, or usefulness of any information, apparatus, product, or process disclosed, or represents that its use would not infringe privately owned rights. Reference herein to any specific commercial product, process, or service by trade name, trademark, manufacturer, or otherwise does not necessarily constitute or imply its endorsement, recommendation, or favoring by the United States Government or any agency thereof. The views and opinions of authors expressed herein do not necessarily state or reflect those of the United States Government or any agency thereof.

DISCLAIMER

Portions of this document may be illegible in electronic image products. Images are produced from the best available original document.

DISCLAIMER

This report was prepared as an account of work sponsored by an agency of the United States Government. Neither the United States Government nor any agency thereof, nor any of their employees, makes any warranty, express or implied, or assumes any legal liability or responsibility for the accuracy, completeness, or usefulness of any information, apparatus, product, or process disclosed, or represents that its use would not infringe privately owned rights. Reference herein to any specific commercial product, process, or service by trade name, trademark, manufacturer, or otherwise does not necessarily constitute or imply its endorsement, recommendation, or favoring by the United States Government or any agency thereof. The views and opinions of authors expressed herein do not necessarily state or reflect those of the United States Government or any agency thereof.

NIPER-392
Distribution Category UC-122

THE EFFECTS OF VISCOUS FORCES ON THREE-PHASE RELATIVE PERMEABILITY

Topical Report

By
D.R. Maloney
S.M. Mahmood
M.M. Honarpour

NIPER--392

DE89 000737

April 1989

Work Performed Under Cooperative Agreement No. FC22-83FE60149

Prepared for
U.S. Department of Energy
Assistant Secretary for Fossil Energy

E. B. Nuckols, Project Manager
Bartlesville Project Office
P.O. Box 1398
Bartlesville, OK 74005

Prepared by
IIT Research Institute
National Institute for Petroleum and Energy Research
P.O. Box 2128
Bartlesville, OK 74005

MASTER

DISTRIBUTION OF THIS DOCUMENT IS UNLIMITED

TABLE OF CONTENTS

Page

Abstract....1
Introduction....1
Literature review....4
Experimental equipment and procedures....9
Saturation measurement procedure....12
Results and discussion....16
Observations and conclusions....23
References....25
Appendix A....26
Appendix B....59
Appendix C....65

TABLES

1. Basic core properties....27
2. Relative permeability results from core no. 11....28
3. Relative permeability results from core no. 12....29
4. Relative permeability results from core no. 13....29
5. Three-phase relative permeability data for core no. 16....30
A-1 Summary of literature review on three-phase relative permeability experiments....46

ILLUSTRATIONS

1. Schemiatic of the X-ray/microwave apparatus for oil and water saturation measurements during three-phase relative permeability experiments....31
2. Steady-state multiphase relative permeability procedures....32
3. Typical saturation profile during a three-phase scan, core 16, test M....33
4. Linear plot of microwave versus x-ray response for several scan positions....33
5. Pulse height distribution curves for core no. 13....34
6. Core no. 13 x-ray calibration for one position with various window settings....34
7. X-ray calibration curves for oil/gas and oil/brine systems....35
8. Semi-log plot of two-phase imbibition and drainage relative permeability data for cores 11, 12, and 13 with viscosities for cores 13, 12, and 11 are 47.8, 4.3, and 1.2-cP oil viscosities of 1.2, 4.3, and 47.8-cP respectively....36
9. Linear plot of two-phase relative permeability data....36
10. The comparison of three-phase relative permeability curves on tertary diagrams between a low and a high oil-phase viscosity system: (A) gas isoperms, 4-cP oil (B) gas isoperms, 47-cP oil (C) brine isoperm, 4-cP oil (D) brine isoperm, 47-cP oil (E) oil isoperm, 4-cP oil (F) oil isoperm, 47-cP oil. The low and high viscosity data were generated on two similar Berea cores. Only those runs are included in which all three phases were mobile....37

ILLUSTRATIONS - Continued

Page

11. Gas, brine, and oil relative permeability isoperms for core 11. Oil viscosities ranged from1.2 to 20.6 cP....38
12. Brine permeability versus brine saturation from three-phase test results, core 11....39
13. Gas permeability versus gas saturation from three-phase....40
14 Microwave scan results for various concentrations of glycerine in water....40
15. Gas, brine and oil relative permeability isoperms from 0.97 cP (solid lines) and 10.8 cP (dashed line) brine viscosity tests, core 16....41
16. Aqueous-phase and soltrol capillary-pressure curves obtained by centrifuge for various concentration of glycerine/brine mixture at 75 °F....42

THE EFFECTS OF VISCOUS FORCES ON THREE-PHASE RELATIVE PERMEABILITY

By D. R. Maloney, S. M. Mahmood, and M. M. Honarpour

ABSTRACT

The overall objective of Three-Phase Relative Permeability Project (BE9) is to develop guidelines for improving the accuracy of three-phase relative permeability determinations. This need is dictated by considerable data scatter and lack of agreement in results reported by all previous studies on this subject. As a result of a literature review, it appears that a better understanding of the role of viscous, gravity, and capillary forces on three-phase flow is required for improvement in measurement methodologies.

This report summarizes previous studies and explains the progress made at NIPER on studying the effect of variations in viscous forces on three-phase relative permeabilities by changing the viscosity of both wetting and nonwetting phases. Significant changes were observed due to viscosity variations. An increase in oil viscosity reduced the relative permeability to gas; an increase in brine (wetting-phase) viscosity reduced the relative permeability to brine. A slight increase in gas relative permeability was also observed. This could be due to the change in interfacial tension and/or irreducible brine saturation. These observations suggest that the viscosities of both oil and water influence three-phase permeability data.

During this study, data scatter was sometimes encountered which was comparable to that of published results. The causes of this scatter are outlined in this report and remedial attempts are discussed, which include methods of improving in situ saturation determination, and use of important operating criteria.

INTRODUCTION

Most reservoir engineering designs, oil recovery forecasts, and feasibility studies of enhanced oil recovery methods incorporate relative permeability data. These data are commonly used in reservoir simulators to

evaluate reservoirs for oil recovery potential. Because of their paramount importance, the accuracy of such predictions is contingent upon the reliability of relative permeability determinations in the laboratory.

One of the most challenging questions faced in laboratory determination of relative permeability is what scale should (or could) the operating conditions for the tests be idealized without affecting the reliability of the measurements. An exact simulation of test conditions often leads to overwhelming operational difficulties, thus compromising accuracy; whereas too much idealization raises disturbing questions about the applicability of laboratory data to reservoir conditions.

Several studies have addressed this issue through tests in which important parameters were varied in dimensionless groups (like capillary number describing the ratio of viscous to capillary forces) or by independently varying individual parameters such as fluid viscosity, flow velocity, fluid interfacial tension (IFT), wettability, pore geometry of the medium, or core dimensions. Many of these studies have shown that changes in capillary number (or other dimensionless groups) or the individual variables within the group (velocity, interfacial tension, and viscosity) affect two-phase relative permeabilities.[1]

The effects of viscous and capillary forces on three-phase relative permeabilities have not been well documented except that the effect of lowering interfacial tension on three-phase relative permeabilities for a brine-oil-surfactant-alcohol system has been reported. No work was ever reported for low interfacial tensions in gas-oil-water systems.

Three-phase relative permeability studies are uncommon because of operational difficulties and complexities in the analysis of results. The advent of high-speed digital computers and recent improvements in laboratory instrumentation for in situ saturation measurements such as computer tomography (CT), X-ray and microwave absorption techniques, gamma-ray attenuation, and nuclear magnetic resonance imaging (NMRI) have improved this situation considerably. Despite these improvements, accurate and reliable measurement of three-phase relative permeability is still experimentally and analytically tedious.

The research on three-phase-flow phenomena, even though limited, has

clearly shown that the regime of fluid saturations in which all three phases are flowing simultaneously is relatively small. Nonetheless, the presence of a third phase, even if immobile, has been shown to influence the transport properties of the other two phases profoundly. The opinion of the authors is that a much better understanding of multiphase flow phenomena can only be obtained when the existing methodologies of three-phase relative permeability measurements are improved for higher accuracy and better reliability.

With this philosophy, NIPER has continued research on three-phase relative permeability determinations for the Department of Energy for the past 4 years under a project titled "Three-Phase Relative Permeabilities." The early goals for this project were to: evaluate the methods of fluid saturation measurement (e.g. volumetric, gravimetric, and resistivity) for their suitability for three-phase relative pemeability determinations; design and assemble equipment for performing accurate three-phase measurements; implement a procedure for testing the validity of test procedures and accuracy/reliability of test equipment; and automate the process such that the important operating parameters are controlled and maintained by a computer during three-phase relative permeability tests.

The highlights of progress and the achievements of this project to date are described below:

- A protocol has been established after successful testing for precise determination of in situ fluid saturations using X-ray/microwave instruments.

- The X-ray/microwave apparatus has been computerized for automatic scanning of cores at predetermined locations.

- Two- and three-phase relative permeability tests on Berea sandstones were performed at ambient conditions and included studies on the effect of viscosity of both brine and oil (wetting-phase and intermediate-wetting-phase, respectively) on three-phase relative permeabilities.

- The use of NMRI for three-phase relative permeability determination has been investigated. It was concluded that a medical type NMRI has limitations for determination of fluid saturations in porous media. However, early attempts at NIPER suggested that a water signal may be differentiated from an oil signal by setting up different inversion times in the inversion recovery sequence. Based on these promising preliminary results, we recommend

that the potential of this technique for estimation of the quantity and spatial distribution of oil and water in cores should be further investigated.

- A power-function parametric model for three-phase relative permeability (TPKR) has been proposed and validated with previously published data. This model contains seven parameters to be estimated for each of the phases present. The model fitted the experimental data throughout the three-phase region with ± 0.52% accuracy.

- A nonmetallic coreholder for high-pressure, high-temperature studies has been fabricated which allows in situ saturation measurements using the X-ray/microwave apparatus for three-phase relative permeability determinations at reservoir conditions.

- Gravimetric, volumetric, and electrical resistivity techniques (i.e. the conventional techniques) were evaluated for accurate determination of fluid saturations during two- and three-phase steady-state relative permeability tests and were found to have serious limitations.

- A black oil simulator has been adapted for analysis of data obtained during two- and three-phase unsteady-state tests. This simulator fits the production data with the model and, thus, backcalculates three-phase relative permeabilities.

Literature Review

Published three-phase relative permeability data were examined to compare the results of various studies. An outline of all published works related to three-phase relative permeability is provided in appendix A. A summary of these studies is provided in table 1. Similar summary tables have also been published by Honarpour et al.,[2] Oak et al.,[3] and Donaldson and Kayser.[4]

Hardly any concensus was found in the literature, either quantitative or qualitative, as to the effect of the presence of a third mobile phase on relative permeabilities. For example, the shape of the isoperms (constant permeability curves) was different on ternary diagrams. The only agreement was in the observation that the saturation envelope on a ternary diagram in which all three phases are mobile is rather small.

The lack of agreement was attributed to the wide variety of operating conditions under which these studies were performed. An attempt was made to

compare the results after grouping these studies on the basis of experimental conditions. Again, no agreement was found either in the shape of isoperms, saturation envelopes, or relative permeability values even for studies with similar test conditions and using "similar" cores (such as Berea sandstone).

After a thorough inspection of all the published literature on this topic, we concluded that further studies are required to demonstrate three-phase relative permeability behavior. It is also apparent that only elaborate and comprehensive studies with good control of frontal stability, hysteresis, and wettability may provide conclusive results. A good understanding of the relative importance of parameters affecting three-phase flow is also necessary.

Some common difficulties encountered in the laboratory determination of three-phase relative permeabilities are reviewed in the following paragraphs. A summary of the important observations reported by all the studies is provided at the end of this section.

Lack of repeatability is quite common in three-phase relative permeability determinations because results are procedure-dependent. First, a reasonably accurate measurement of saturations when more than two phases are involved is difficult. Material-balance techniques for saturation determination are generally shown to be inaccurate when pore volumes of injectant are large, especially for steady-state tests; therefore, in situ saturation measurement techniques are required. Other relative permeability determination techniques, i.e., displacement tests (unsteady-state) and centrifuge methods, yield only approximate results because of the simplifying assumptions necessary for obtaining mathematical solutions. In the centrifuge method, the relative permeability to gas cannot be determined. In displacement tests, one of the three phases must be immobile. The results from all techniques are influenced by the state of initial fluid saturations.

Another problem is the lack of scaling criteria for three-phase flow tests. Capillary, viscous, and gravity forces influence irreducible saturation levels. End-point saturations have a pronounced effect on the shape of isoperms. Without guidelines for operating conditions, handling experimental problems such as capillary end effects becomes difficult.

A major limitation in performing three-phase relative permeability

tests is the time required to perform experiments. The equilibration process is quite slow in most instances. To obtain a complete set of data for ternary diagrams, a long time period (weeks to months, depending on the transmissivity of the core/fluids system) is required. From reviewing the literature, it appears that many investigators performed their studies without allowing enough time for complete steady-state flow equilibration.

The most serious problem appears to be the saturation hysteresis effect. As relative permeabilities are saturation-history dependent, the manner in which an experiment is conducted has an effect on the accuracy of results. While it is relatively easy to either increase or decrease the saturation of a phase in a two-phase system, it is intrinsically difficult to change core saturation conditions in a controlled sequence during three-phase flow experiments. In the displacement process, the core is completely saturated with a wetting phase, e.g. water, and oil is introduced. When gas is subsequently injected for the determination of unsteady-state three-phase relative permeabilities, it causes the oil saturation to decrease. Therefore, oil saturation does not change monotonically, rather, it first increases then decreases. This introduces hysteresis effects which make the relative permeability values dependent on initial saturations and direction of saturation changes. Several techniques have been tried in which the saturation of oil is held constant, but in those cases, it has not been demonstrated convincingly that relative permeability values would be similar as if all three phases were mobile.

To cover the entire saturation envelope for steady-state, three-phase flow tests on a ternary diagram, the saturation of all three phases cannot be changed monotonically (because the total saturation cannot exceed 100%) without cleaning or replacing the core. Cleaning has often been shown to alter wettability and pore geometry and thus affect relative permeability results Replacing a core with a similar sample is not always possible because cores from the same block have exhibited different flow behavior. In both situations, considerable data scatter can be expected. To avoid changes, studies have performed complete tests on the same sample without cleaning, such that the saturation of two of the phases is monotonic, whereas the saturation of the third phase (usually wetting phase) is allowed to change direction in small cycles. This procedure has considerable merit, provided it

can be ascertained early in the investigation that the third phase is not significantly influenced by hysteresis effects.

One common problem encountered during these studies was interpreting isoperms, i.e., the lines of constant relative permeability. All investigators except one[3] have performed experiments without any control for maintaining fixed relative permeability values while changing saturations. Experiments in which relative permeability values were obtained by randomly changing saturation conditions generally yielded insufficient data to draw well-defined isoperms on ternary diagrams. The situation is further complicated due to data scatter because of operational difficulties described in the above paragraphs. Typically, the scatter in relative permeability data on ternary diagrams is so great that the isoperms cannot be drawn accurately by manual interpolation without significant individual bias. Some studies have avoided this bias by using computer-fitting subroutines (e.g. multivariate curve-fitting), but the results are still not unique because of operator bias in defining arbitrary constraints. Several curve-fitting algorithms have been suggested for interpolation (and extrapolation) of laboratory data, with schemes ranging in complexity from simple linear fit to multiple power-law functions.[5]

To avoid the need for interpolation, some researchers have held one of the phases stationary using semipermeable membranes. In some recent studies,[3] experiments have been performed on computer-automated equipment to yield preassigned constant relative permeability values for each phase. This is done by continuously adjusting the saturations of all three phases (by varying the injection rates) to maintain the value of the relative permeability of a phase constant. An attempt is made, even though not entirely successful, to keep the changes in saturation monotonic. In such schemes, the data scatter is reduced significantly, and the analysis of data is straightforward.

Several important developments have been reported recently due to renewed interest in this area. Grader and O'Meara[6] presented a method of analysis in which all three phases can be mobile concurrently, so that one of the phases does not have to be at residual saturation conditions. They used this method to analyze data generated by flowing three liquid phases through a glass beadpack. Their method, however, has yet to be supported by independent studies on consolidated cores and in systems in which one of the flowing

phases is a gas. Oak et al.[3] have recently performed experiments using fully automated, computer-controlled equipment where rates are adjusted to attain saturations which will yield fixed values of isoperms. Good control of hysteresis was possible in this study. Their published results are the only source in which actual data points are shown without curve-fitting. Full-automation of three-phase relative permeability equipment appears to offer definite advantages in obtaining accurate data.

A summary of the state-of-the-art review is presented as follows:

1. In most studies, there was considerable data scatter which was classified by most researchers as characteristic scatter of three-phase relative permeability measurements.

2. Most studies used some type of data-smoothing or curve-fitting techniques to produce meaningful data.

3. Many studies reported significant end-effects in the core.

4. The three-phase flow region on ternary diagrams was shown to be small.

5. The shape of the isoperms (curves of equal permeability values) on ternary diagrams varied in most studies. Some researchers reported that the relative permeability of each phase was a function of its own saturation, whereas others believed relative permeability for each phase to be a function of all three saturations. In most cases, however, relative permeability to brine was reported to be a function of brine saturation alone, while oil relative permeability was thought to be a function of the saturations of all three phases. The relative permeability to gas could be interpreted either way because the curvature observed in some studies was too small to be considered beyond experimental error.

6. The true shapes of isoperms could not be described conclusively from published data. Although some studies showed large curvatures in the isoperms covering the entire region of the saturation envelope, the curvature in the zones where all three phases were flowing was rather small. If the brine and gas data points were curve-fitted, excluding points outside the three-phase flow region, a straight line could just as well be drawn within experimental accuracy.

7. Hysteresis played an important role in both steady-state and

unsteady-state tests.

8. Most studies ignored the capillary pressure effect in calculation of relative permeability isoperms, and this distorted relative permeability values close to irreducible saturations.

EXPERIMENTAL EQUIPMENT AND PROCEDURES

The dimensions and petrophysical properties of the Berea sandstone cores used in this study are outlined in table 2. The brine permeability of these cores ranged from 500 to 700 md, and their porosity, from 22 to 25%. These cores were machined with rectangular cross sections of 2-cm thickness (width) and 5 cm height. The cores were fired at 1,000 °F, for 24 hr to stablize clays. Each core was encapsulated in an epoxy-resin gauze jacket to confine flow. The nonmetalic jacketing material was required in order to use microwave techniques for monitoring brine saturations. As no overburden pressure was applied to the cores, the maximum allowable pore pressure for these epoxy resin-coated cores was 150 psig. High-viscosity fluids, high flow rates, or long cores were avoided to keep the pore pressure within a 5 to 50 psi working pressure range.

Experiments began with clean, dry samples. Steady-state flow conditions were established by simultaneous injection of test fluids at constant rates. After reaching equilibrium, the saturations of oil and brine were measured by using X-ray and microwave techniques. Flow rate and pressure drop measurements, along with core/fluid data, were used in Darcy's law to calculate effective permeabilities to each phase, which were then normalized to obtain relative permeability values. Saturations were changed by adjusting the ratio of injection rates of each fluid.

Further details of the procedure are described in the following sections. An outline of the experimental setup is shown in figure 1. The step-by-step procedure is shown in the box diagram of figure 2. Expanded details of each of these steps are included in appendix B.

Core Cleaning Procedure

Before saturating the core completely with a liquid or gas phase, the core was first cleaned in situ with pentane and CO_2 and dried with N_2. First, the pentane in equilibrium with CO_2 was injected for about 2 hr at an upstream pressure of 10 to 15 psi maintained by a CO_2 vessel (cylinder). Carbon dioxide alone was then injected for 1½ hr at 10 to 15 psi injection pressure. Finally, N_2 injection was continued overnight at 10 to 15 psi pressure to dry the core.

Core Saturating Procedure

The procedure for saturating the cores using a high-pressure saturation apparatus was similar to the one described by Worthington.[7] In this method, an epoxied core and a small glass thimble are placed in a high-pressure vessel in such a fashion that any gas bubbles released from the core are trapped in the thimble. The vessel is subjected to alternating cycles of strong vacuum and low-pressure CO_2 injection. After the last vacuum cycle, the pressure vessel is flooded with degassed brine and then slowly pressurized to 1,000 psi by pumping additional brine into the vessel. After 24 hr, the pressure is slowly released from the vessel. Immediately after removing the end cap from the vessel, the glass thimble is examined for the presence of any bubbles which, if present, indicate incomplete saturation. The saturation is deemed complete when no bubbles are present in the glass thimble. This procedure has shown to be quite successful in achieving complete saturation in cores, as demonstrated by CT scans taken before and after core saturation.

In this work, some cores were saturated by in situ injection techniques which consisted of injecting CO_2 for several hours at 10 to 15 psi and then injecting brine to displace CO_2. Complete saturation was assumed when the steady-state flow of brine was established and continued for at least 2 hours. Table 3 identifies the cleaning procedure used for different tests.

Selection of Viscosities and Flow Rates

To examine the effects of flow rates and viscosities on three-phase relative permeability, it was desirable to perform experiments over a wide range of rates and viscosities. Excessive flow rates or high viscosities were avoided to protect the mechanical integrity of the epoxy-resin core jacket.

Low flow rates were avoided to limit the manifestation of end effect. A compromise in pressure and rate limits was therefore made using the following criteria:

$$R_e = \frac{bWk}{6.33 \times 10\mu A} \leq 0.1 \qquad (1)$$

where:

b = turbulence factor, ft^{-1}
W = mass flow rate lbm/sec
k = permeability, md
μ = viscosity, cP
A = cross sectional area, ft^2

$$\Delta p \leq 50 \text{ psig (max pressure drop)} \qquad (2)$$

To approximate pressure drops at a given rate using Darcy's law, the effective permeability to each phase was approximated using previously published results in similar cores.

Tests were performed to examine the effect of flow rate on the apparent permeability of the cores. In these tests, the rate was gradually increased. No change in permeability was noticed initially; however, a reduction in permeability was observed upon achieving a certain high rate. This rate is referred to as critical rate. The reason for this reduction in pemeability was presumed to be due to the migration of fine particles across the pores, which eventually results in the trapping of particles in small pore throats. However, it is also possible that some changes in the rigidity of the core holder took place. Nonetheless, all experiments were performed at rates much below critical rates in order to obtain reliable data.

Criteria for Attainment of Equilibrium Conditions

Before relative permeability measurements were considered to be of acceptable quality, the following criteria had to be met to ensure that

steady-state test conditions were attained:

(a) at least 5 PV of brine and oil had been injected;
(b) nonmonotonic pressure fluctuations hadbecome stable within 1% of the average pressure drop for at least 1 hr; and
(c) consecutive X-ray and microwave scans had demonstrated no saturation fluctuation for at least 1 hr.

SATURATION MEASUREMENT PROCEDURE

Oil and water saturations were measured in situ by using X-ray absorption and microwave attenuation techniques, respectively. For two-phase tests, X-ray and microwave techniques were directly comparable since both monitored oil or brine saturation are a linear function of attenuation. Figure 3 shows a typical saturation distribution between the pressure measuring taps during a three-phase, steady-state flow test.

The system was occasionally calibrated by comparing X-ray and microwave derived saturation measurements with those determined by material balance and gravimetric methods. The accuracy of saturation measurements was within ±1% for X-ray and ±3% for microwave techniques. Satisfactory results from microwave techniques were obtained only by using epoxy-resin-coated cores of up to 2 cm thickness because of limitations on the capability of the microwave detector used.

To minimize gravity segregation of the test fluids, an arrangement was made whereby the cores were set horizontally during the test, except their orientation was switched temporarily from horizontal to vertical during X-ray and microwave scanning. This was accomplished by installing hinged stands which allowed the 2-cm widths to be oriented parallel to the horizontal plane during flow tests.

Quality Control for Saturation Measurements

Because of the permanent enclosure of the core in epoxy-resin/gauze coatings, gravimetric techniques were not applicable for saturation determination because of the heavy weights involved. Volumetric methods also showed severe limitations because of the large dead volumes compared to the

pore volumes. Thus, the accuracy of saturation measurements by X-ray and microwave instruments was not easily checked by an independent method.

However, the reliability of saturation measurements by X-ray and microwave was assured by cross-plotting the microwave and X-ray intensity responses for at least four central scan positions (7 mm apart) and plotting the results as natural logarithms of X-ray response versus natural logarithms of microwave response, as shown in figure 4. Since the microwave response should be linear with respect to the brine saturation and the X-ray response should be linear with respect to the oil saturation, it can be inferred that the microwave and X-ray responses should be linearly related for a two-phase oil/brine system. Thus, a linear trend in data such as that shown in figure 4 was indicative of the reliability of X-ray/microwave measurements.

To further improve the quality of measurements, X-ray and microwave scans were taken several times at each saturation level until repeatable results were obtained that agreed to within 1% over a 2-hr period. Separate calibration curves were developed for each scan position along the entire length of each core at 7 mm intervals.

Saturation Measurements by X-ray Technique

Before each test, the alignment of X-ray source and detector was checked (and corrected when required) by inspecting the image of the projected beam on a Polaroid film affixed to the surface of the detector.

To improve the accuracy of saturation measurements, only the intensity of a narrow band of wavelengths in the X-ray spectrum was measured, the rest was filtered out before reaching the detector (counter) by an instrument called a pulse-height analyzer (PHA). This narrow band of wavelengths is called a "window setting." A narrow window setting improves the linearity of calibration curves, but it decreases the signal-to-noise ratio; thus, an optimum has to be experimentally determined for the test core by comparing the accuracy of saturation measurements with different window settings at several saturation levels.

The procedure for determining the optimum window setting is as follows. First, the X-ray power level is selected so that the intensity of X-rays transmitted through the core, when fully saturated with the test fluid, is

enough to be easily detected by the detector. A cross section of the core is then scanned at dry, fully brine-saturated, conditions and at residual water saturation conditions. The PHD curves are then constructed, as shown in figure 5 for a typical Berea sandstone core (No. 13). From these plots, the peak intensity considering all saturation levels is determined, which is shown to be occuring around a pulse amplitude of 48% in figure 5. Next, the core is scanned again using various window settings around the pulse amplitude yielding the peak intensity (e.g. 48% in fig. 5), and the results are plotted as oil saturation versus natural log of emergent X-ray intensity (typical plots are shown in figure 6). The window setting providing the best degree of linearity in the oil saturation versus X-ray intensity calibration curve is selected, which incidently is the narrowest window setting (46/53) in figure 6.

Saturation Measurements by Microwave Technique

The microwave technique was selected for brine saturation measurements because it does not require a tagging agent. It has been shown to be effective for three-phase relative permeability experiments. However, it imposed certain limitations on experimental techniques because of the requirement of a nonmetalic coreholder.

Metallic coreholders are unsuitable for saturation measurements by the microwave technique because of high energy absorption and reflection. Therefore, the cores were jacketed with epoxy resin (reinforced with gauze), and tests were performed without confining pressure. In the absence of confining pressure, the core jacket was prone to bursting or peeling off under excessive pore pressures. To avoid such mechanical failures, which cause significant time losses, a limitation of 50 psi was imposed as the maximum pore pressure.

Because of the low sensitivity of the microwave detector, the thickness of the test cores had to be limited to a maximum of 2 cm. The optimum microwave penetration was experimentally found to be through the cores with rectangular shape of crosssection; hence, rectangular cores were used exclusively.

Bypassing and radiation of microwave energy above and below the cores during microwave scans were often problemetic, even though lens-focused sensing and receiving antennas were used. Such energy reaches the microwave

receiving antenna (and detector) without penetrating cores and thus impairs the accuracy of saturation measurements, especially at high water saturations when most of the energy is absorbed and only a small percentage of energy emerges through the core. To overcome this problem, shields of microwave absorbing material were affixed to prevent nonemergent microwaves from reaching the receiving antenna.

A new microwave coreholder was tested and found satisfactory for conducting relative permeability measurement using the X-ray/microwave technique under high confining pressure. Details of the testing procedure of this coreholder are outlined in appendix B.

Improvements in X-ray/Microwave Calibration Procedure

In using microwave and X-ray absorption techniques for saturation determination, a calibration curve for either the X-ray or microwave must be established before the test is started. This is done by scanning the core twice -- under saturation conditions in which the saturation of the phase of interest is 0% and after it is fully saturated with the test fluid to be monitored. The intensity responses during the test are converted to saturation readings by interpolating through the calibration curve. Since the calibration curve is established when the core is either unsaturated or fully saturated with the test fluid, an error is introduced when a third phase of noticeable absorbing capacity is also present.

The microwave technique is predominantly sensitive to brine saturation. The presence of oil or gas does not introduce noticeable errors. On the other hand, the X-ray technique is sensitive to both liquids and the lack thereof; i.e. absorption in untagged brine can often be significant, even though it is much smaller than the absorption in tagged oil (e.g., with 10% iodododecane). Therefore, the use of an X-ray calibration curve established by using only an oil/gas system may be prone to errors. The following method was used to handle this problem, which allows for the accounting of X-ray absorption in brine as well.

Instead of using only an oil/gas X-ray calibration curve, an additional calibration curve (oil/water) was also established. This was done before the tests by scanning the core three times, i.e. at comletely dry conditions, after fully saturating it with tagged oil, and after fully saturating it with

untagged brine. These three scans generated two lines representing X-ray calibration curves for oil/gas and oil/brine systems, as shown in figure 7 for a typical Berea sandstone core. Such calibration curves were plotted for every position in the core of which the saturation had to be measured.

During three-phase-flow systems, a measured X-ray intensity response will theoretically represent any saturation condition between the two calibration curves, as shown, for example, in figure 7. In this figure, a measured value of the natural log of intensity of 11.1 [Ln(I) = 11.1] could correspond to saturations anywhere between 33 and 50%. However, the brine saturation is determined independently by the microwave technique, which helps in determining the true oil saturation by interpolating between the two calibration curves. Such interpolation is based on the principal of linear proportionality between oil/gas and oil/brine calibration curves. This can be mathematicaly expressed as:

$$S_o = (S_o)100\%w\text{-}X\text{-}ray + \frac{(S_w)microwave - (S_o)100\%w\text{-}X\text{-}ray}{(S_o)dry\text{-}X\text{-}ray - (S_o)100\%w\text{-}X\text{-}ray}$$

In virtually all tests during FY88, saturating the core completely with oil was avoided to maintain the original wettability of the core. In those situations, the X-ray response for 100% oil saturation condition was calculated, by using the correlation between microwave and X-ray responses. Using the calculated value of the response for 100% oil saturation, X-ray calibration curves were constructed for each scan position. These calibration curves based on a calculated response are called synthetic curves. To validate these curves, irreducible water and residual oil saturation conditions were attained in the core, and saturations were determined by both X-ray and microwave techniques. The saturation values determined by X-ray using the synthetic calibration curve were in excellent agreement with the values determined by the microwave, showing the validity of synthetic X-ray calibration curves.

RESULTS AND DISCUSSION

The results presented here show the shapes of the three-phase relative permeability isoperms on ternary diagrams and the effects of variations in wetting-phase and oil-phase viscosities on three-phase relative

permeabilities. The data were obtained as a result of an ongoing research project at NIPER, and as such, include results from the earlier studies performed during fiscal years 1985-87, the preliminary results of which have been reported.[8] However, the previous results were reevaluated to obtain additional information. A brief summary of important observations is provided in the following two paragraphs. More detail is provided in the following sections.

It was found that Berea sandstone cores from the same quarried block can have significantly different relative permeability values, and the saturation envelopes in ternary diagrams can also show dissimilar behavior. The brine and oil relative permeabilities were found to be independent of the oil-phase viscosity. However, the relative permeability to gas was considerably lower for a higher viscosity oil, suggesting the possibilities of coupled flow in the gas channels.

Oil and gas relative permeabilities were essentially independent of the wetting-phase viscosity. Brine isoperms demonstrated a significant change when glycerine was used to viscosify brine. However, the changes in brine composition, e.g. oil-brine interfacial tension, might have affected the wetting characteristics of the cores.

Effect of Oil-Phase (Nonwetting) Viscosity on Two-Phase Relative Permeability

Three Berea cores (No. 11, 12, and 13) were used to study the effect of oil phase viscosity on two-phase relative permeability. Imbibition and drainage water-oil relative permeabilities were determined using white mineral oils of 1.2, 4.3, and 47.8 cP viscosities. Brine viscosity was 1.02 cP for each test. The data are plotted in figures 8 and 9. These figures show some scattering, which is much smaller in oil relative permeability than in brine relative permeability data. The scattering in brine relative permeabilities may be primarily due to different degrees of microporosity that are presumed to exist in different Berea cores. No effect of oil viscosity on oil-water relative permeabilities was found. However, the irreducible brine saturation level seemed to be lowered by using a higher viscosity oil.

Effect of Oil-Phase (Nonwetting) Viscosity on Three-Phase Relative Permeability

The properties of the four Berea sandstone cores used in this study are listed in table 1. All four cores were obtained from the same quarried block, and their absolute gas permeabilities ranged from 590 to 690 md. Cores 1 and 4 showed quite different behavior in three-phase relative permeability when compared to cores 2 and 3. The major differences were in residual saturations when all three phases were present. The saturation envelopes on ternary diagrams for three-phase flow were not identical in size and location. However, cores 2 and 3 showed similar behavior. The exact reason for this dissimilarity is not known. Since the cores were cut from the same block and had approximately the same absolute permeability and porosity, they were less likely to differ in pore structure, or pore size distribution. The cores were never cleaned during these experiments; thus, there was little possibility that wettability changes would have occurred.

Note that the effective permeability data were normalized with respect to brine absolute permeabilities for calculation of relative permeability values. When the results were analyzed, considerable data scatter was observed, similar to the observations by some previous investigators. This scatter was perhaps caused by operational difficulties inherent in three-phase flow experiments. Manual interpolation was found to be difficult and impractical because of the extent of data scatter. A three-dimensional interpolation was required for each ternary diagram. The data were plotted by graphical contouring with the help of a three-dimensional interpolation technique described previously.[9] Some of the contour plots required additional smoothing. Because of the computer interpolation and smoothing involved for some of the curves, the values should be considered approximate. However, the trends are definite, and qualitative comparison is quite justified.

The effect of changes in oil-phase viscosity on three-phase relative permeability is shown in figure 10 in which the ternary diagrams for the 4-cP oil system (core 2) and the 47-cP oil system (core 3) are compared. As mentioned previously, cores 2 and 3 showed similar characteristics. A total of 28 three-phase flow runs were performed on core 2, and 60 similar runs were performed on core 3. The graphical contouring technique could be used

successfully to draw isoperms of values only when enough experimental data were available. When the number of data points for a specific value was small, the resulting curves were found to be ambiguous.

As shown in the ternary diagrams, the brine isoperms are linear and have approximately the same value for both the 4- and 47-cP systems. This implies that the wetting-phase relative permeability depends only on its own saturation. It also implies that the wetting-phase relative permeability is independent of oil-phase viscosity.

The oil isoperms for both 4- and 47-cP oil systems are concave towards the 100% oil apex, indicating that the relative permeability to oil is a function of all three saturations. The 10% isoperm in the 4-cP system appears to occur at a slightly lower saturation, but the other data points (not shown as isoperms because of being few in number) for higher relative permeability values (such as 20%) indicate that the relative permeability to oil for a 4-cP oil is the same as that of 47-cP oil. Thus, oil viscosity does not seem to affect the relative permeability to either oil or brine.

The gas isoperms are also concave towards the 100% gas appex, indicating that gas relative permeability depends on all three saturations. However, unlike brine and oil relative permeabilities, the gas isoperms are seen to occur at approximately 15 to 20% higher gas saturations for a 47-cP oil than for a 4-cP oil. Of the many theories that explain this behavior, one that seems plausible is that a different flow mechanism is involved when a higher viscosity oil is present, possibly a slug-type flow. Equally likely is the possibility that the pore-level physics of the flow mechanism described in the literature may be inadequate to describe three-phase flow.

Repeatability of Experiments

To determine the repeatability of the above experiments, three-phase relative permeability tests were performed on an entirely different system. The Berea core (No. 11) and the cleaning/initial saturation procedures were changed, and the oil viscosity was varied from 1.2 to 20.6-cP in these tests. The isoperms for this test are shown in figure 11.

As in previous tests, the brine isoperms were linear (fig. 11B) and had the same values for three oils of viscosities in the range of 1.2 to 20.6-cP,

conforming the previous test results that the wetting-phase relative permeability is dependent on its own saturation and independent of oil-phase viscosities. As a matter of fact, the three-phase brine relative permeabilities were not much different from that of the two-phase values, as evident by comparing two- and three-phase brine relative permeability data in the saturation range investigated. Also, the imbibition and drainage relative permeabilities of brine were almost identical showing that the wetting-phase relative permeability is not significantly influenced by hysteresis. Consequently, much less scatter was observed in brine relative permeability data (fig. 12).

Oil isoperms also showed repeatable behavior. Isoperms for 1.2- and 9.4-cP viscosity oils were not only similar but also had concave curvature toward 100% oil apex (fig. 11C), confirming that the relative permeability to oil is a function of the saturations of all three phases. Two additional observations were made: (1) a faster increase in oil relative permeabilities was observed with increasing oil saturation above 20% gas saturation, and (2) at higher oil saturations, oil isoperms showed substantial scattering, especially for the 20.6-cP oil. Much of the scattering is believed to be due to the hysteresis phenomenon.

Whereas the effect of oil-phase viscosity on both oil and brine relative permeabilities was quite repeatable in these independent tests, some difficulties were encountered for gas relative permeabilities. The data scatter in gas permeability (as shown in figure 13) was too large to draw nonlinear curves with reasonable accuracy. Therefore, straight lines were drawn on ternary diagrams for gas relative permeabilities (fig. 14). This linearity in gas isoperms, however, may not indicate that gas relative permeability depends on its own saturation; it merely implies that the true curvature of the isoperms cannot be determined due to the scatter, especially since gas isoperms are reported to have small curvatures. For similar reasons, it is not possible to outline the effect of an order of magnitude variation in oil viscosity from core 11 data.

The affluent observations during tests on core 11 support the earlier hypothesis that a different type of flow mechanism is involved in the presence of high-viscosity oils. The relative permeability tests using high-viscosity oils encountered slug-type gas flow at the producing end, associated with

large pressure fluctuations. This observation was in sharp contrast to the low-viscosity oil tests in which gas flow was continuous. Besides, during high-viscosity oil tests, the gas relative permeability at higher gas saturations did not increase with an increase in gas saturation (fig. 13). This is attributed to the onset of plug-type flow at high gas saturations in high-viscosity oil tests.

Effect of Brine-Phase (Wetting) Viscosity on Three-Phase Relative Permeability

The effect of wetting phase viscosity on three-phase relative permeability was examined by conducting a series of steady-state, three-phase relative permeability tests on an epoxy-jacketed Berea core exposed to a net overburden pressure of 35 atm. Test results showed the wetting phase viscosity to have a pronounced effect on wetting-phase relative permeabilities, but minimal effect on nonwetting-phase relative permeabilities.

In these tests, white mineral oil and nitrogen were the two nonwetting phases, whereas the wetting phase was either brine (1.0% NaCl in deionized water) or a mixture of glycerine and brine (1.0% NaCl) yielding a room temperature viscosity of 10.8-cP. Saturations of aqueous-phase oil and gas were determined by microwave, X-ray, and material balance (by difference), respectively. Calibration tests showed that microwave attenuation is predominantly influenced by the brine content of the aqueous phase, thus, the microwave technique can be used effectively for aqueous phase saturation determination. Figure 14 shows the ratio of emergent to incident microwave energy for various concentrations of glycerine in brine. The approximately linear relationship between Ln (b/a) and glycerine concentrations higher than 30% is a positive check on the applicability of the microwave technique for these tests.

After completing the three-phase-flow experiments using the 0.97-cP brine, the core was flooded with the brine to approach residual oil and gas saturations. The core was then flooded with the 10.8-cP brine to miscibly displace the 0.97-cP brine. It was flooded with oil, and finally, it was flooded with glycerine again. Microwave and X-ray scans were taken after each flood. A new microwave calibration curve for 10.8-cP brine was developed

using a similar approach to that previously described. Three-phase flow conditions were re-established, and additional sets of three-phase relative permeability and saturation data were recorded.

The oil, brine, and gas isoperms on ternary diagrams are presented in figure 15. Because of the difficulties inherent in this type of three-phase relative permeability tests (as mentioned previously), considerable manipulation of data was required to arrive at these isoperms; hence, the results were used for qualitative interpretations only. The isoperms in this test were drawn manually, not by computer graphical contouring techniques as in tests described previously.

As in the previous tests, brine relative permeabilities appeared to be influenced by brine saturations alone, as shown in figure 15B. However, the increase in brine (wetting-phase) viscosity from 0.97 to 10.8 cP led to an increase in brine relative permeabilities. There was no significant change in the trends of oil isoperms due to the more than 10-fold increase in wetting phase viscosity (fig. 15C). There was a slight tendency for gas isoperms to decrease because of the increase in wetting-phase viscosity (fig. 15A).

It is important to realize that the change in brine viscosity was accompanied by changes in interfacial tension. The measurements by spinning drop tensiometer showed the interfacial tension between the 10.8-cP brine and the oil to be 26 dynes/cm, whereas it was 51.5 dynes/cm between the brine and the oil. The drop in interfacial tension to about one-half could also have significantly affect wettability characteristics and, consequently, fluid distribution. The capillary-pressure/brine-saturation curves (fig. 16) obtained by centrifuge also indicate that the concentration of glycerine changes the irreducible brine saturation.

Even though it is highly desirable to separate the two effects, i.e. the effect of variations in viscosity and interfacial tension, it is very difficult (if not impossible) to find two fluids of significantly different viscosities but similar interfacial characteristics. Nevertheless, the capillary-pressure curves can be quite helpful in this situation. Figure 16 indicates that increasing the concentration of glycerine also increases residual brine saturation -- an indication that the system has become more water-wet. If such would be the case, the relative permeability to brine would decrease because the wetting phase preferentially flows through the

smallest channels and offers more resistance to flow. On the contrary, the relative permeability to brine increased by increasing glycerine concentration. This strongly suggests that it was due to the increase in viscosity and not due to change in interfacial tension. This is also supported by the fact that no change in oil relative permeabilities was observed. The decrease in gas relative permeability might again be explained on the basis of plug-type flow encountered during the use of high-viscosity brine.

OBSERVATIONS AND CONCLUSIONS

The following observations and conclusions were made as a result of this steady-state experimental study performed on Berea sandstones. The results were obtained after the accuracy of relative permeability measurements was considerably improved by refining the saturation calibration methodology in X-ray/microwave techniques and by introducing a high-pressure, high-temperature nonmetallic coreholder.

1. Similarity in flow behavior of cores from same origin: Samples obtained from the same quarried block showed dissimilar characteristics. For example, the saturation envelopes in the ternary diagrams for three-phase flow were not identical. The brine relative permeabilities for these cores were significantly different, presumably because of variations in degrees of microporosities that may exist in different cores.

2. Size of the three-phase flow envelope: The three-phase flow region was small, but the presence of gas as a third phase, even when it was immobile, reduced the oil relative permeability drastically.

3. Shape of the isoperms in three-phase flow: The relative permeability to brine was a function of only its own saturation because the brine isoperms in a ternary diagram were linear. The gas isoperms showed such a small concavity toward the 100% gas saturation apex that it could have been considered to be linear. However, the oil relative permeabilities were a function of all three saturations. The oil isoperms in the ternary diagram were concave towards their 100% saturation apex.

4. Effect of oil-phase viscosity on two-phase flow: Relative permeabilities to both oil and water were independent of oil-phase viscosity.

5. Effect of oil-phase viscosity on three-phase flow: Both brine and oil relative permeabilities were independent of the oil-phase viscosity, but the gas relative permeabilities were lowered when higher viscosity oil was used. This reduction in gas permeability may be attributed to the slug-type flow encountered during the high-viscosity oil tests.

6. Effect of wetting-phase viscosity on three-phase flow: Oil isoperms were essentially independent of the wetting-phase viscosity. Brine isoperms showed a significant change when glycerine was used to viscosify brine. A reduction in oil-brine interfacial tension was observed for high-viscosity brine due to the addition of glycerine, but the decrease in brine relative permeabilities was attributed to the increase in viscosity. Gas relative permeabilities were also increased for high-viscosity brine, which was again attributed to the plug-type flow.

7. Repeatability of tests: The results on the effect of oil-phase viscosity were repeated by independent tests, and reasonable agreement was obtained. Similarly, the gas and oil isoperms during tests conducted for the effect of wetting-phase and nonwetting-phase viscosity variations were similar under similar conditions.

8. Reason for data scattering: The data scattering observed more significantly in oil relative permeability data was believed to be caused by hysteresis.

ACKNOWLEDGMENTS

This work was performed for the U. S. Department of Energy under Cooperative Agreement DE-FC22-83FE60149. Special thanks are due to Nicida Maerefat, Ravi Parmeswar and Alan Brinkmeyer for generating all previous laboratory data that were reanalyzed and presented in this report. The authors also thank Min K. Tham, Aaron Cheng, Paul Stapp, and Bill Linville of NIPER and E. B. Nuckols of the DOE Bartlesville Project Office for their valuable suggestions and recommendations. Our appreciation is also extended to Willis Waldorf for assisting in experimental data gathering and to Edna Hatcher for typing this manuscript.

REFERENCES

1. Delshad, Mojdeh. Measurement of Relative Permeability and Dispersion for Micellar Fluids in Berea Rock. M.S. Thesis, U. of Texas at Austin, Dec. 1981.

2. Honarpour, M. Relative Permeability of Petroleum Reservoirs. CRC Press Inc., Bata Raton, FL, 1986.

3. Oak, M. J., L. E. Baker, and D. C. Thomas. Three-Phase Relative Permeability of Berea Sandstone. Pres. at the SPE/DOE Enhanced Oil Recovery Symposium. Tulsa, Apr. 17-20, 1988. SPE/DOE paper 17370.

4. Donaldson, E. C. and G. W. Dean. Two- and Three-Phase Relative Permeability Studies. BuMines RI 6826, 1966, 23 pp.

5. Honarpour, M., S. M. Mahmood. Relative Permeability Measurements: An Overview. SPE Tech. Today Series, J. Pet. Tech., Aug. 1988.

6. O'Meara, D. J., Jr. and W. O. Lease. Multiphase Relative Permeability Measurements Using an Automated Centrifuge. Pres. at the SPE Ann. Tech. Conf. and Exhibit., San Francisco, Oct. 5-8, 1983. SPE paper 12128.

7. Worthington, A. A Technique for Detecting Incomplete Saturation of Cores. J. Pet. Tech., Dec. 1978, pp. 1716-1717.

8. Parmeswar, R., N. L. Maerefat, and A. Brinkmeyer. Preliminary Results on the Effect of Fluid Viscosity on Three-Phase Relative Permeability. Topical Report, Natl. Inst. for Petrol. and Energy Research. Department of Energy Report No. NIPER-296, 1987.

9. Parmeswar, R., and N. L. Maerefat. A Comparison of Methods for the Representation of Three-Phase Relative Permeability Data. Pres. at the 56th California Regional Meeting, Oakland, Apr. 2-4, 1986, pp. 151-157.

10. Leverett, M. C. and W. B. Lewis. Steady Flow of Gas-Oil-Water Mixtures Through Unconsolidated Sands. Trans., AIME, v. 142, 1941, pp. 107-116.

11. Reid, S. The Flow of Three Immiscible Fluids in Porous Media. PhD Thesis, Chem. Eng. Dept., U. of Birmingham, UK, 1956, 168 pp.

12. Snell, R. W. The Saturation History Dependence of Three-Phase Oil Relative Permeability. J. Inst. Pet., v. 49, Mar. 1963, pp. 81-84.

13. Saraf, D. N. and I. Fatt. Three-Phase Relative Permeability Measurement Using a Nuclear Magnetic Resonance Technique for Estimating Fluid Saturation. Soc. Pet. Eng. J., v. 7, Sept. 1967, pp. 235-242; Trans., AIME, v. 240, 1967, pp. 235-242.

14. Schneider, F. N. and W. W. Owens. Sandstone and Carbonate Two- and Three-Phase Relative Permeability Characteristis. Soc. Pet. Eng. J., Mar. 1970, pp. 75-84, SPE paper 2445.

15. Caudle, B. H., R. L. Slobod, and E. R. Brownscombe. Further Developments in the Laboratory Determination of Relative Permeability. Trans., AIME, v. 192, 1951, pp. 145-150.

16. Van Spronsen, E. Three-Phase Relative Permeability Measurements Using the Centrifuge Method. Pres. at the SPE/DOE Third Joint Symp. on Enhanced Oil Recovery, Tulsa, April 4-7, 1982. SPE/DOE paper 10688.

17. Corey, A. T., C. H. Rathjens, J. H. Henderson, and M. R. J. Wyllie. Three-Phase Relative Permeability. J. Pet. Tech, v. 8, Nov. 1956, pp. 63-65; Trans., AIME, v. 207, 1956, pp. 349-351.

18. Sarem, A. M. Three-Phase Relative Permeability Measurements by Unsteady-State Method. Soc. Pet. Eng. J., v. 6, Sept. 1966, pp. 199-205; Trans., AIME, v. 237, 1966, pp. 199-205.

19. Guckert, L. G. Gamma Ray Absorption Method of Measuring Gas Saturation and Its Application to Three-Phase Relative Permeability Studies. PhD Thesis, Texas A&M University, 1968.

20. Grader, A. S. and D. J. O'Meara Jr. Dynamic Displacement Measurements of Three-Phase Relative Permeabilities Using Three Immiscible Liquids. Pres. at the 63rd SPE Ann. Tech. Conf. and Exhibit. Houston, Oct. 2-5, 1988. SPE paper 18293.

TABLE 1. - Basic core properties

Core no.	k_{air}, md[1]	k_{brine}, md	Porosity, %	Dimensions, cm		
				L	W	H
1	--	550	21.4	15.25	2.70	3.92
2	687	--	22.5	7.70	2.69	3.87
3	680	--	25.2	7.50	2.69	3.87
4	690	--	22.7	7.70	2.67	3.88
11	562	560	22.3	15.47	1.61	4.90
12	549	515	21.2	15.16	2.01	4.87
13	586	586	22.9	15.28	1.98	4.90
16	--	270	--	14.20	2.20	5.20

[1]Klinkenberg corrected.

TABLE 2. - Relative permeability results from core no. 11

k_L = 560 md

μ_w = 1.02 cP, μ_o = 1.20 cP, μ_g = 0.0176 x 10^{-2} cP

Two-phase water[1]/oil

s_w	s_o	k_{rw}	k_{ro}
0.065	0.349	5.18×10^{-2}	5.66×10^{-3}
0.674	0.326	5.65×10^{-2}	6.18×10^{-4}
0.660	0.340	4.57×10^{-2}	1.99×10^{-2}
0.654	0.346	4.83×10^{-2}	2.10×10^{-2}
0.629	0.371	4.82×10^{-2}	1.61×10^{-1}
0.573	0.427	1.73×10^{-2}	1.83×10^{-1}
0.530	0.470	6.73×10^{-3}	2.56×10^{-1}
0.500	0.500	8.31×10^{-3}	3.16×10^{-1}
0.610	0.390	2.98×10^{-2}	8.53×10^{-2}
0.605	0.395	2.90×10^{-2}	$8.29c10^{-2}$
0.632	0.368	4.41×10^{-2}	3.92×10^{-2}
0.639	0.361	3.09×10^{-2}	2.74×10^{-2}
0.665	0.335	5.09×10^{-2}	9.75×10^{-3}

[1]1% by weight NaCl brine.

TABLE 3. - Relative permeability results from core no. 12

k_L = 515 md

μ_w = 1.02 cP, μ_o = 4.30 cP, μ_g = 0.0176×10^{-2} cP

Two-phase water[1]/oil

s_w	s_o	k_{rw}	k_{ro}
0.590	0.410	4.0×10^{-2}	8.6×10^{-2}
0.566	0.434	3.8×10^{-2}	1.8×10^{-1}
0.536	0.464	2.2×10^{-2}	2.0×10^{-1}

[1]1% by weight NaCl brine.

TABLE 4. - Relative permeability results from core no. 13

k_L = 586 md

μ_w = 1.02 cP μ_o = 47.8 cP

Two-phase water[1]/oil

s_w	s_o	k_{rw}	k_{ro}
0.564	0.436	9.18×10^{-3}	1.44×10^{-1}
0.531	0.469	4.03×10^{-3}	1.89×10^{-1}
0.471	0.529	2.65×10^{-3}	3.72×10^{-1}

[1]1% by weight NaCl brine.

TABLE 5. - Three-phase relative permeability data for core no. 16

K_L = 370 md

μ_w = 0.973 cP (A-G), 10.8 cP (H-M); μ_o = 1.2 cP, μ_g = 0.0176 cP

Test	S_w	S_o	S_g	k_{rw}	k_{ro}	k_{rg}
A	0.548	0.286	0.166	2.075E-02	2.635E-02	4.364E-04
B	0.523	0.379	0.098	1.199E-02	3.970E-02	2.400E-04
C	0.492	0.326	0.182	1.159E-02	1.216E-02	2.022E-04
D	0.506	0.316	0.178	1.226E-02	2.109E-02	1.102E-04
E	0.508	0.306	0.186	1.629E-02	1.203E-02	2.478E-04
F	0.489	0.297	0.214	1.317E-02	2.025E-02	1.115E-04
G	0.470	0.286	0.244	1.062E-02	2.641E-02	9.970E-05
H	0.407	0.295	0.297	1.087E-02	1.653E-02	1.612E-04
I	0.419	0.349	0.232	1.183E-02	1.608E-02	1.121E-04
J	0.445	0.339	0.215	1.315E-02	1.407E-02	1.368E-04
K	0.426	0.354	0.220	1.148E-02	1.428E-02	1.324E-04
L	0.456	0.335	0.209	1.827E-02	1.276E-02	1.083E-04
M	0.452	0.323	0.225	1.90E-02	1.642E-02	1.041E-04

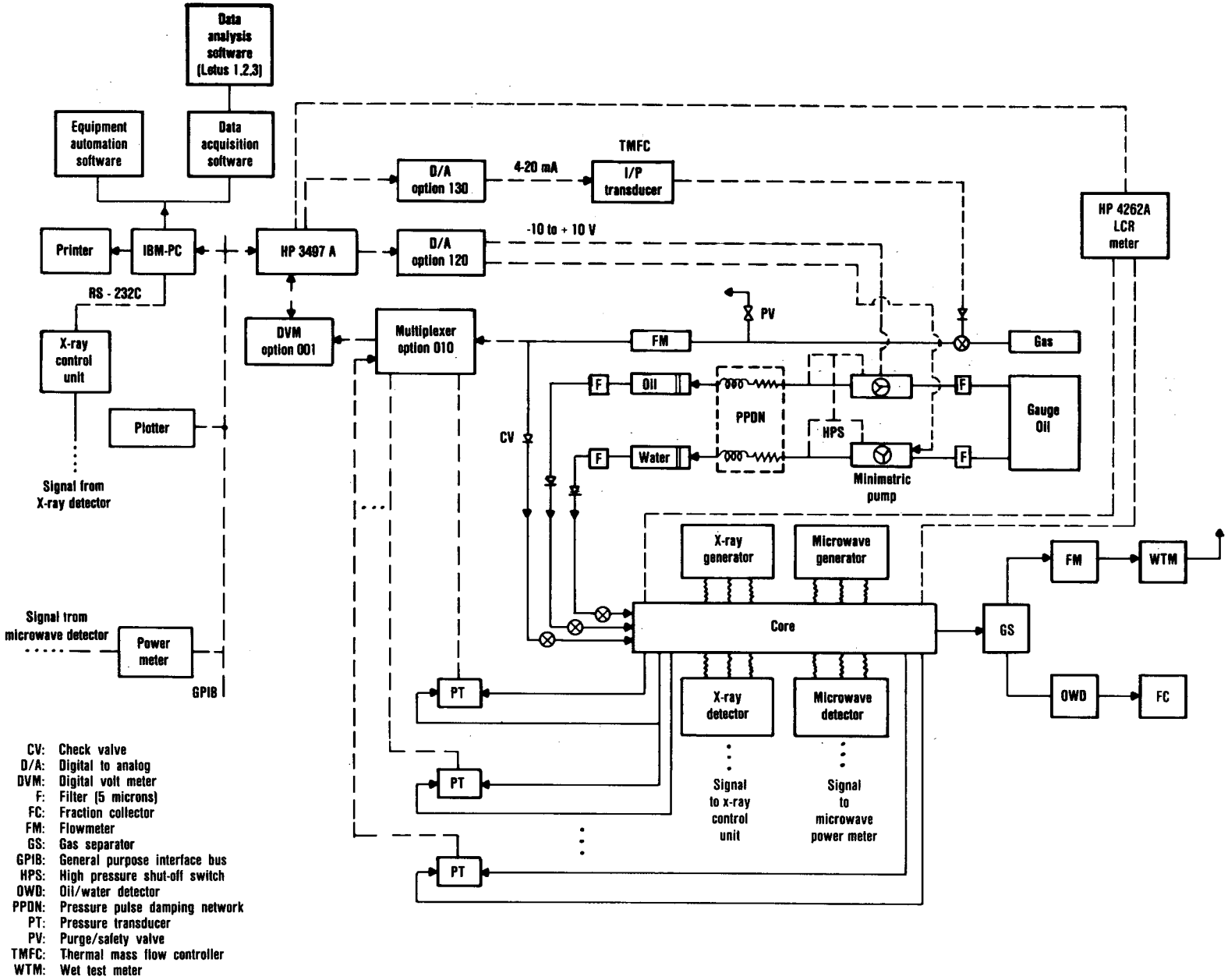

FIGURE 1. - Schematic of the X-ray/microwave apparatus for oil and water saturation measurements during three-phase relative permeability experiments.

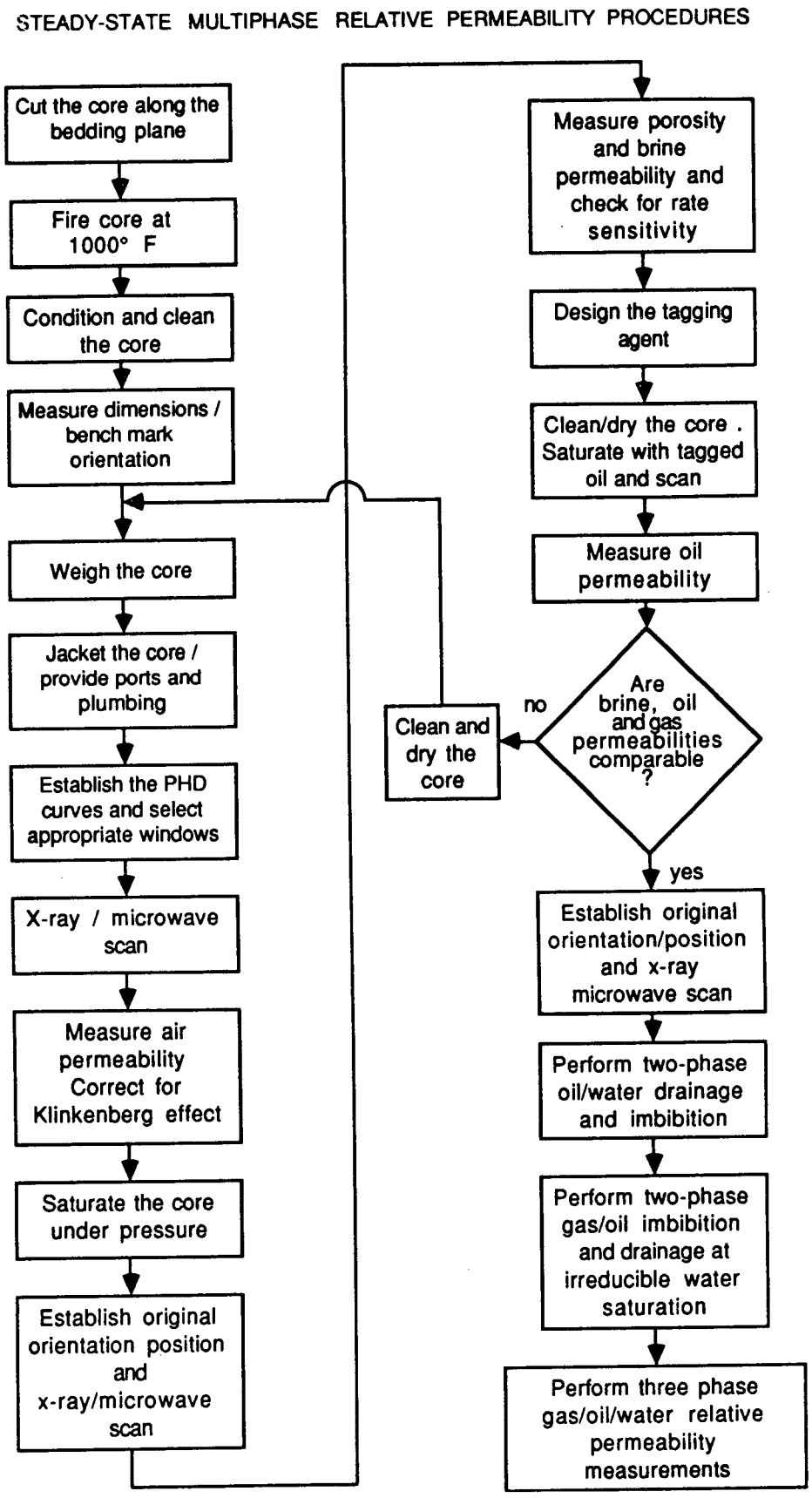

FIGURE 2. - Steady-state multiphase relative permeability procedures.

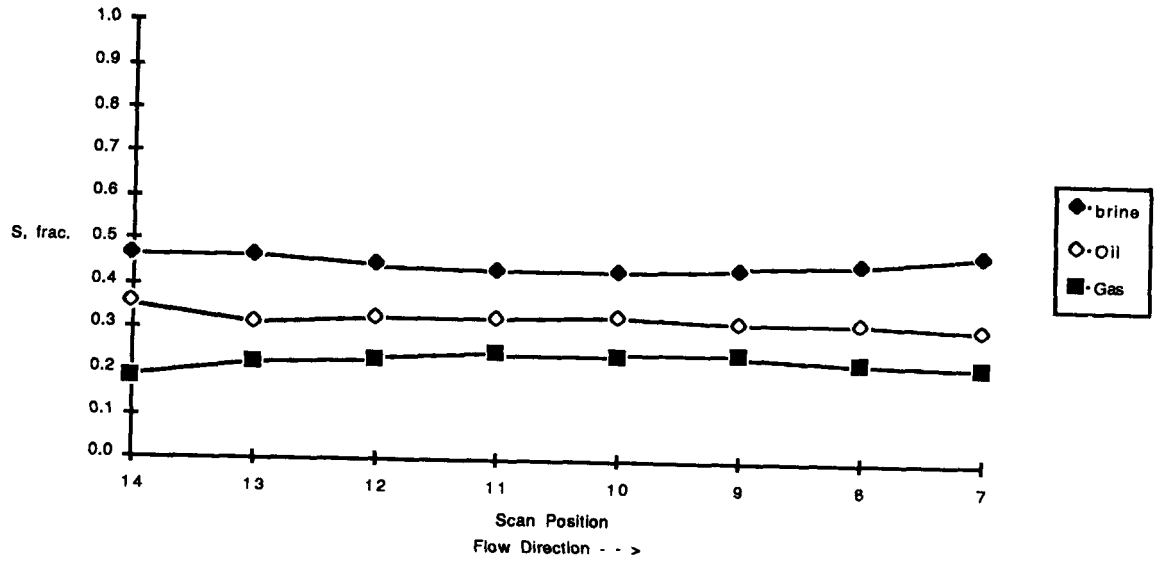

FIGURE 3. - Typical saturation profile during a three-phase scan, core 16, test M.

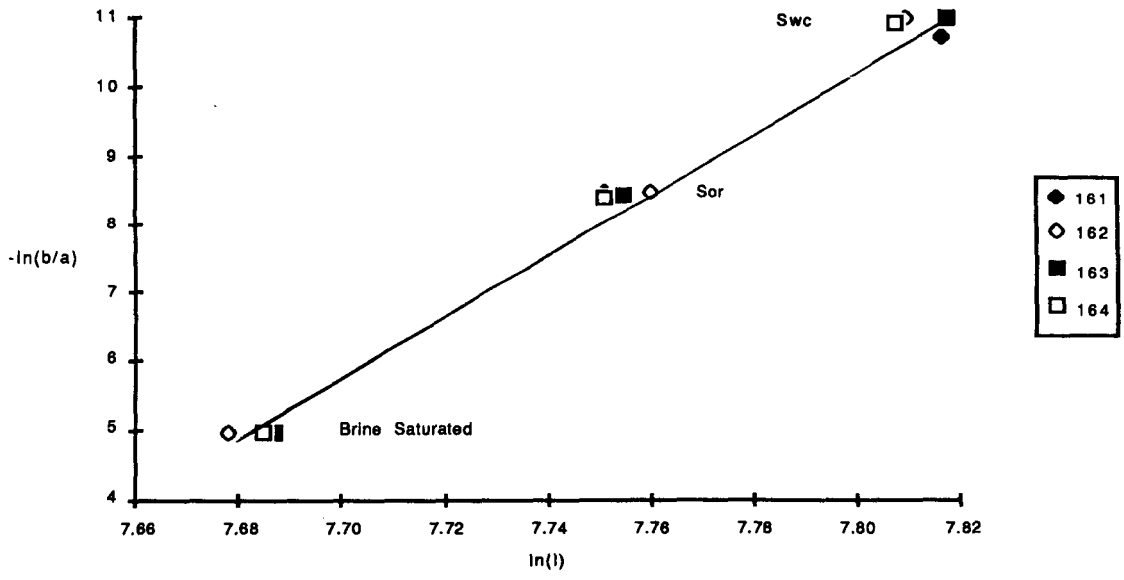

FIGURE 4. - Linear plot of microwave versus x-ray response for several scan positions.

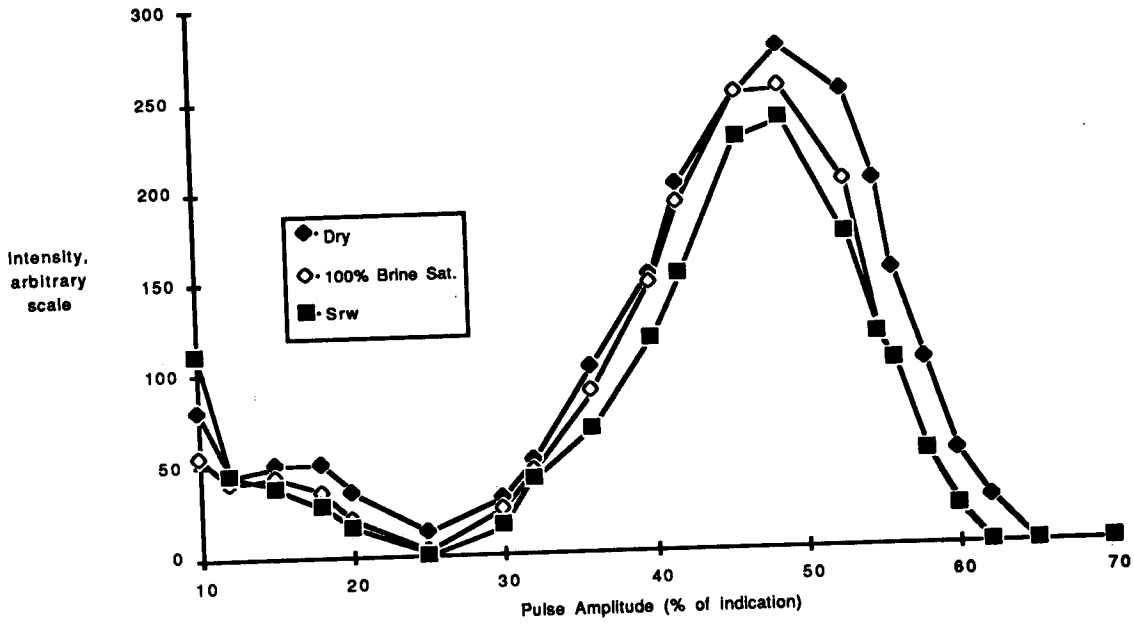

FIGURE 5. - Pulse height distribution curves for core No. 13.

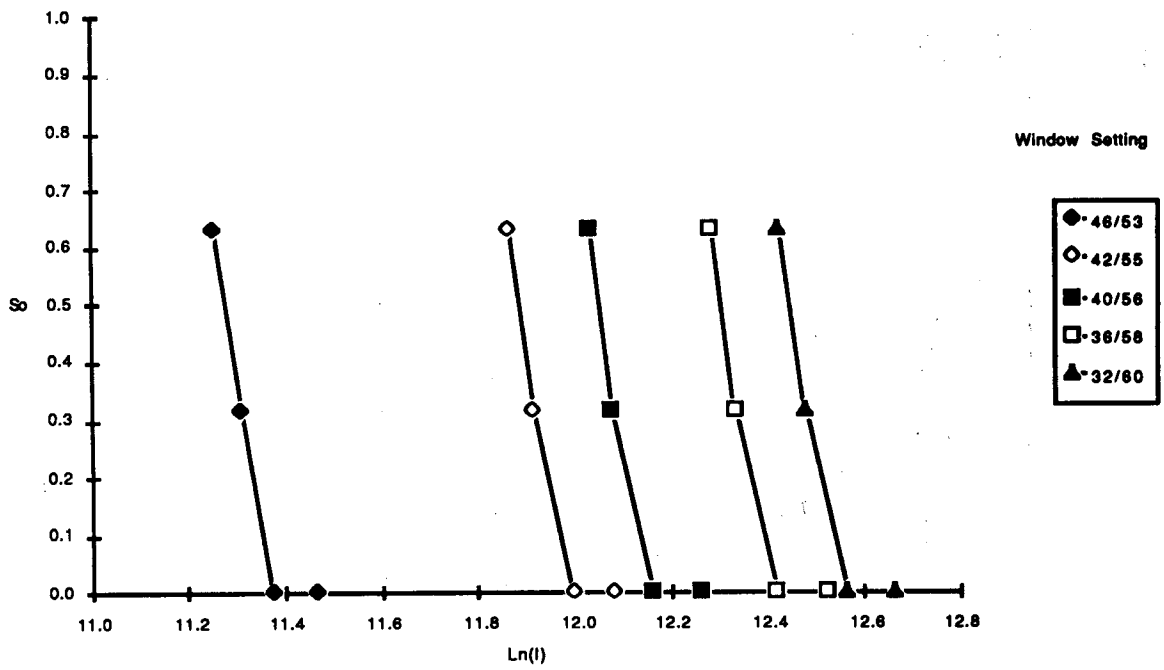

FIGURE 6. - Core No. 13 x-ray calibration for one position with various window settings.

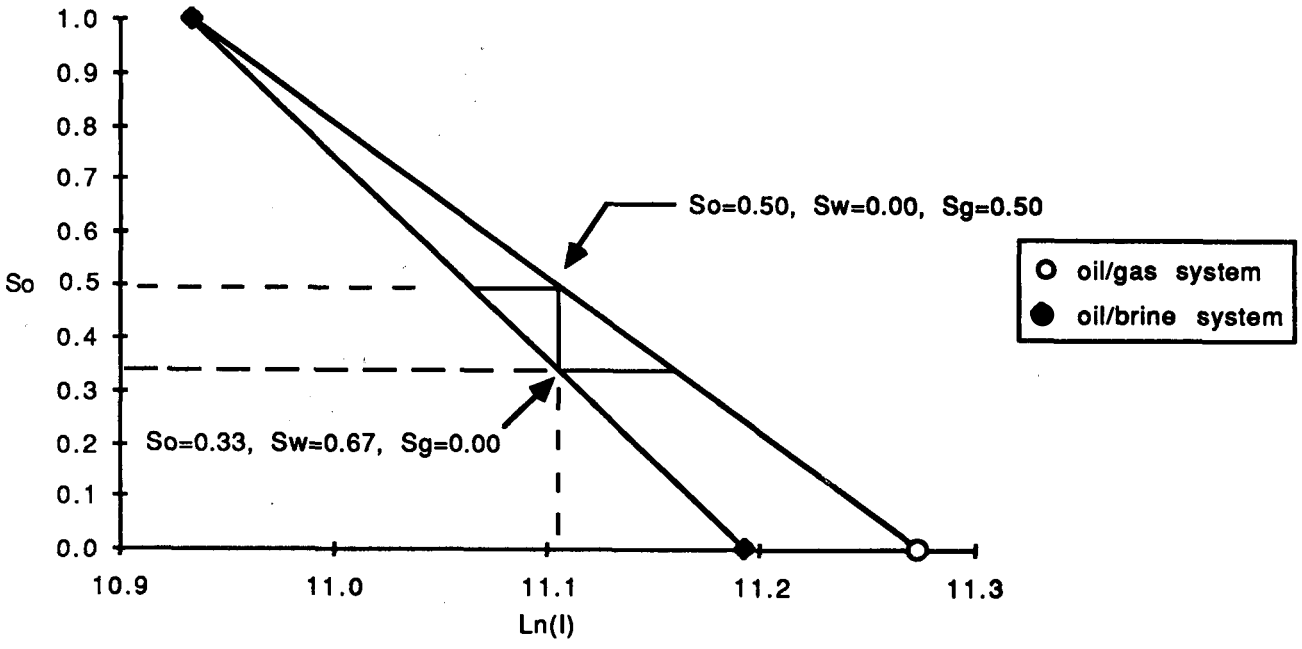

FIGURE 7. - X-ray calibration curves for oil/gas and oil/brine systems.

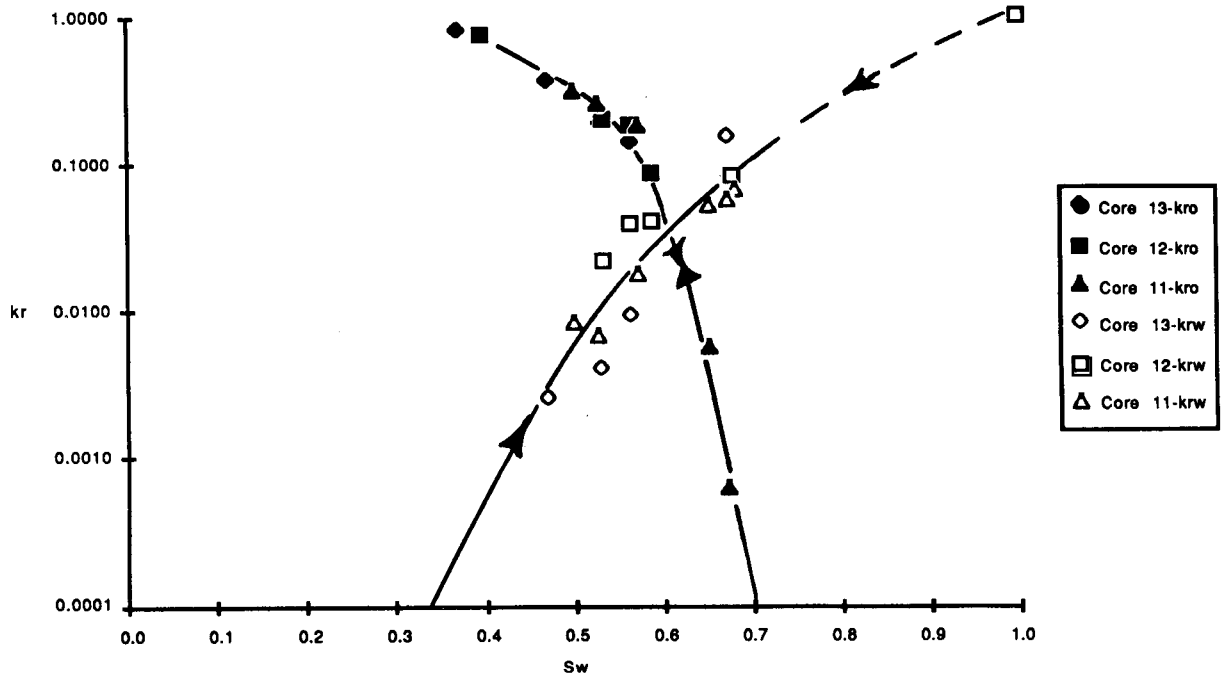

FIGURE 8. - Semi-log plot of two-phase imbibition and drainage relative permeability data for cores 11, 12, and 13 with viscosities for cores 13, 12, and 11 are 47.8, 4.3, and 1.2-cP oil viscosities of 1.2, 4.3, and 47.8-cP respectively.

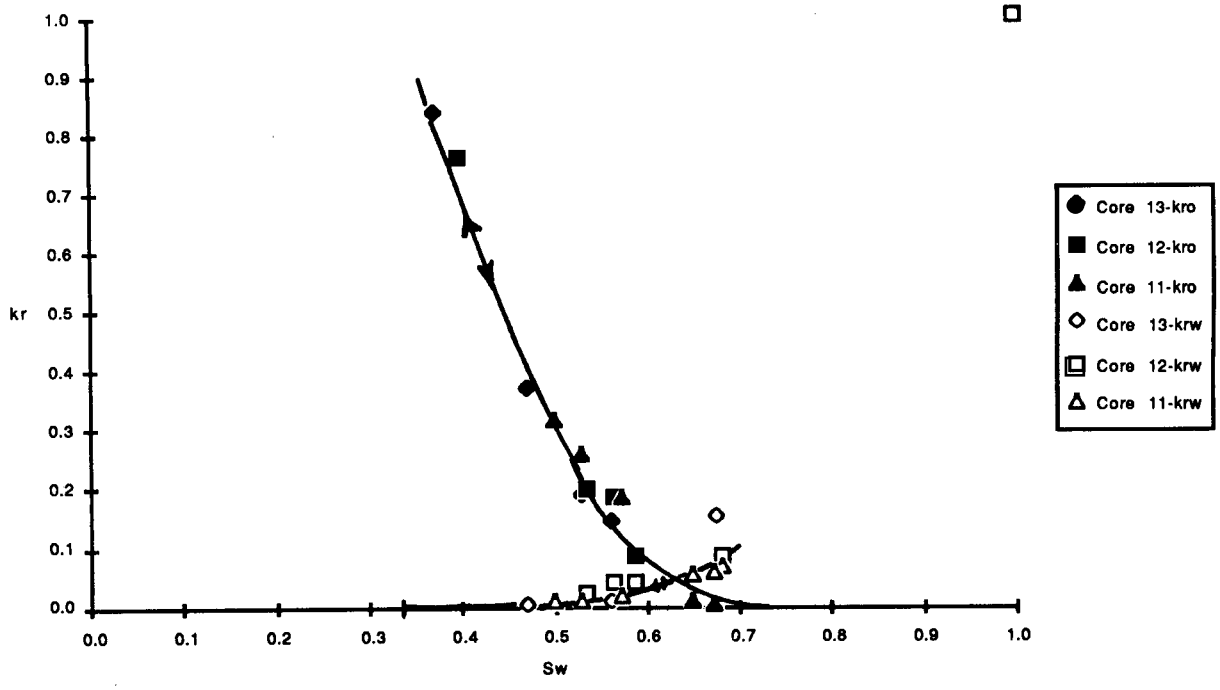

FIGURE 9. - Linear plot of two-phase relative permeability data.

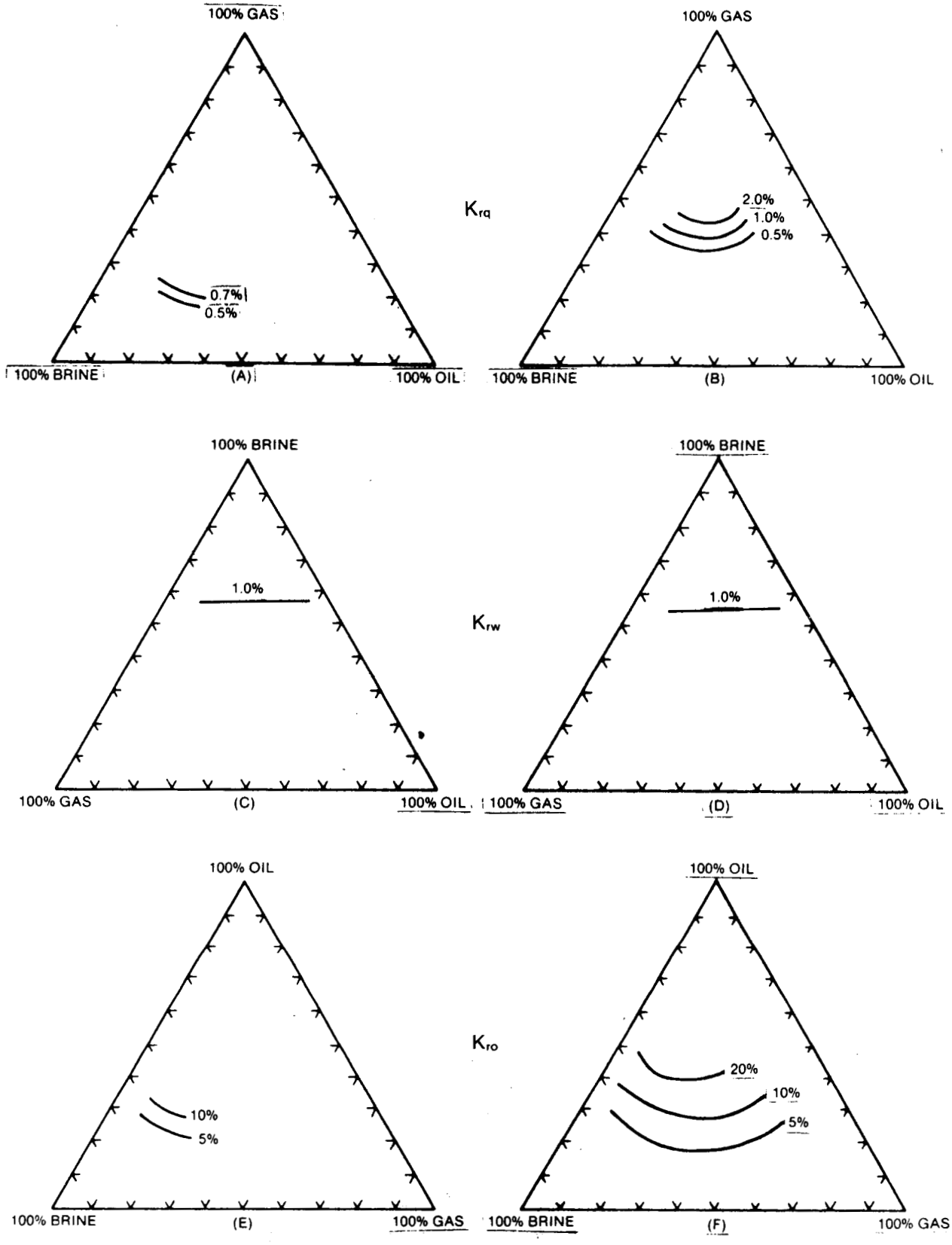

FIGURE 10. - The comparison of three-phase relative permeability curves on tertary diagrams between a low and a high oil-phase viscosity system: (A) gas isoperms, 4-cP oil (B) gas isoperms, 47-cP oil (C) brine isoperm, 4-cP oil (D) brine isoperm, 47-cP oil (E) oil isoperm, 4-cP oil (F) oil isoperm, 47-cP oil. The low and high viscosity data were generated on two similar Berea cores. Only those runs are included in which all three phases were mobile.

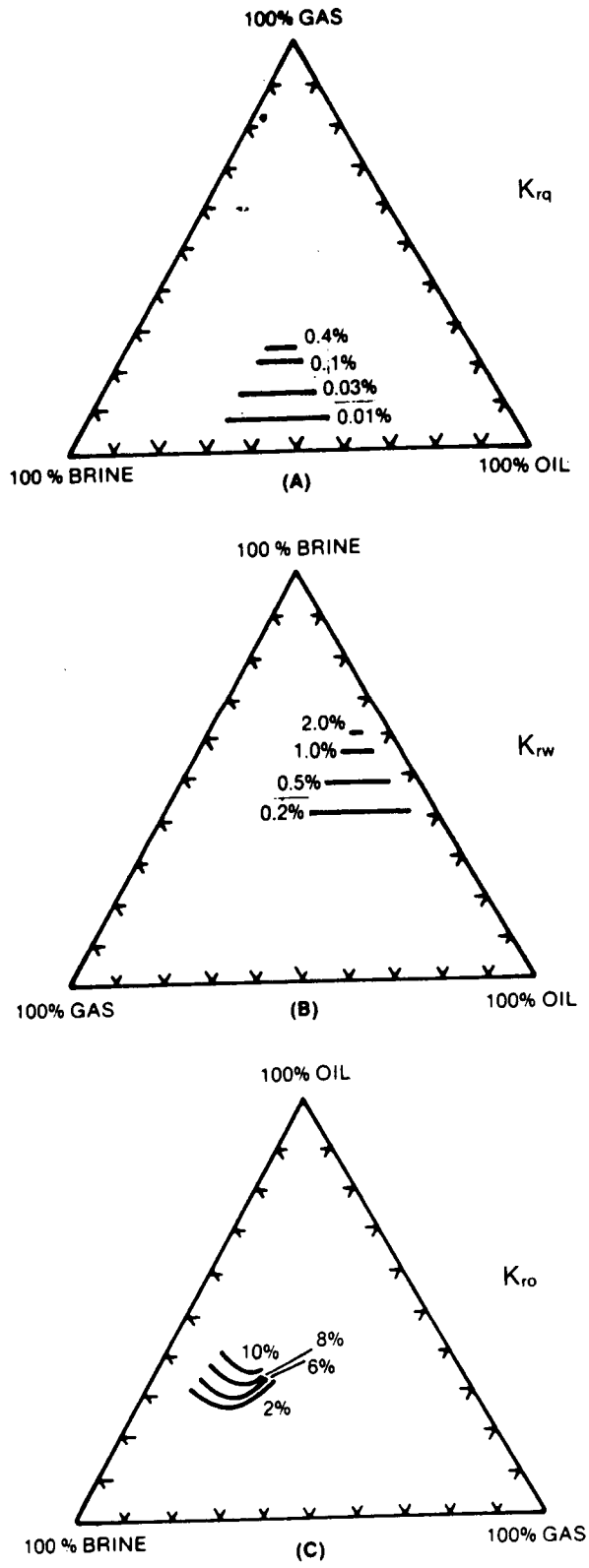

FIGURE 11. - Gas, brine, and oil relative permeability isoperms for core 11. Oil viscosities ranged from 1.2 to 20.6 cP.

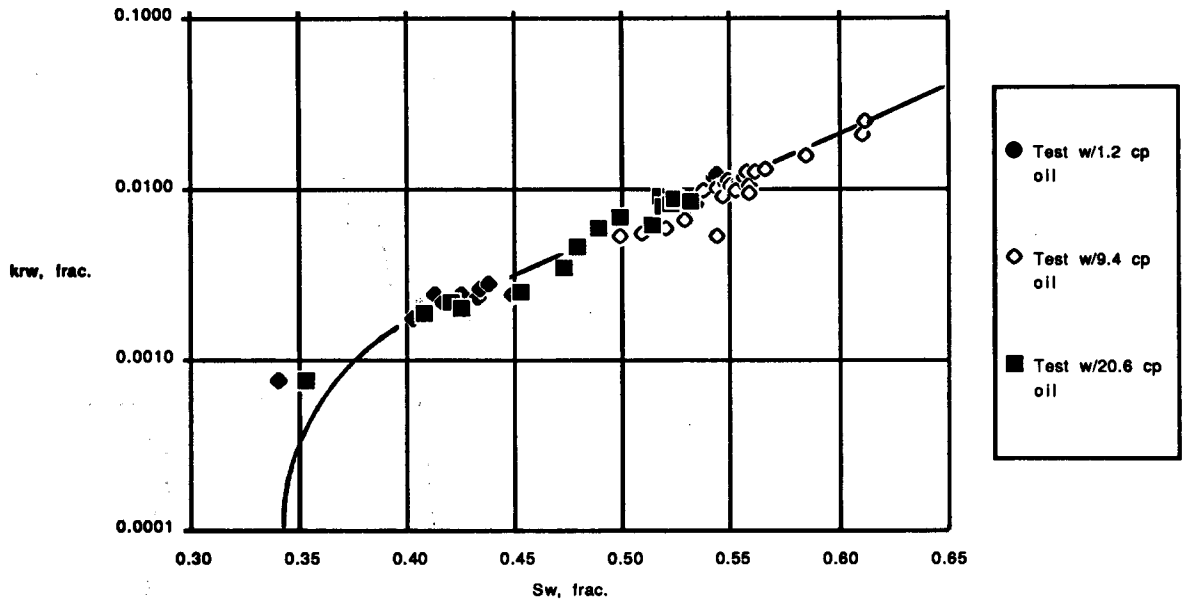

FIGURE 12. - Brine permeability versus brine saturation from three-phase test results, core 11.

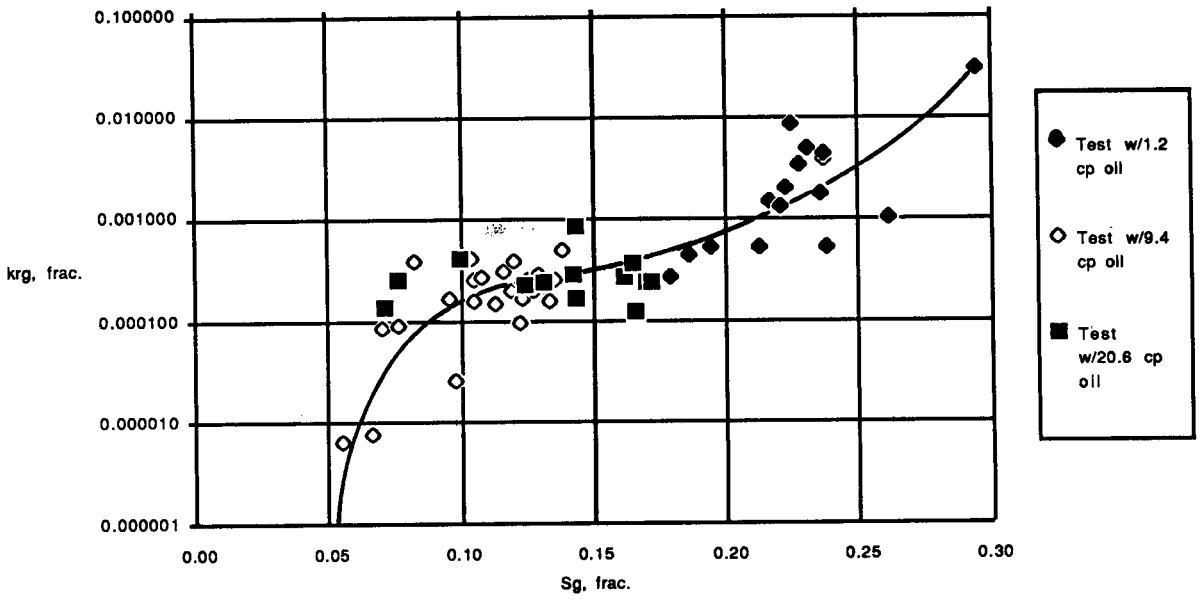

FIGURE 13. - Gas permeability versus gas saturation from three-phase test results, core 11.

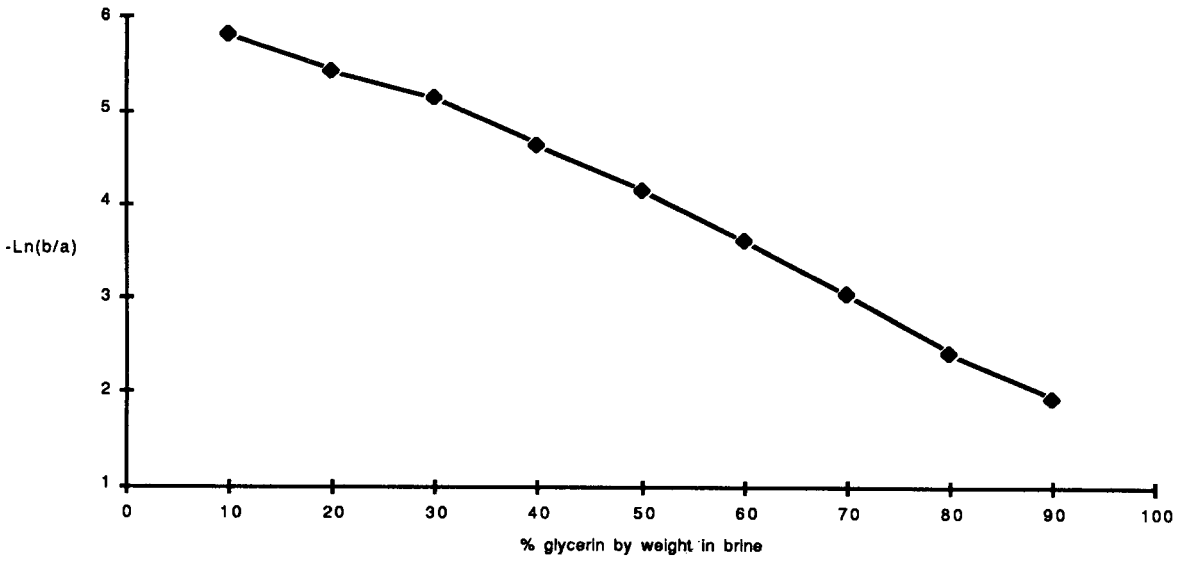

FIGURE 14. - Microwave scan results for various concentrations of glycerine in water.

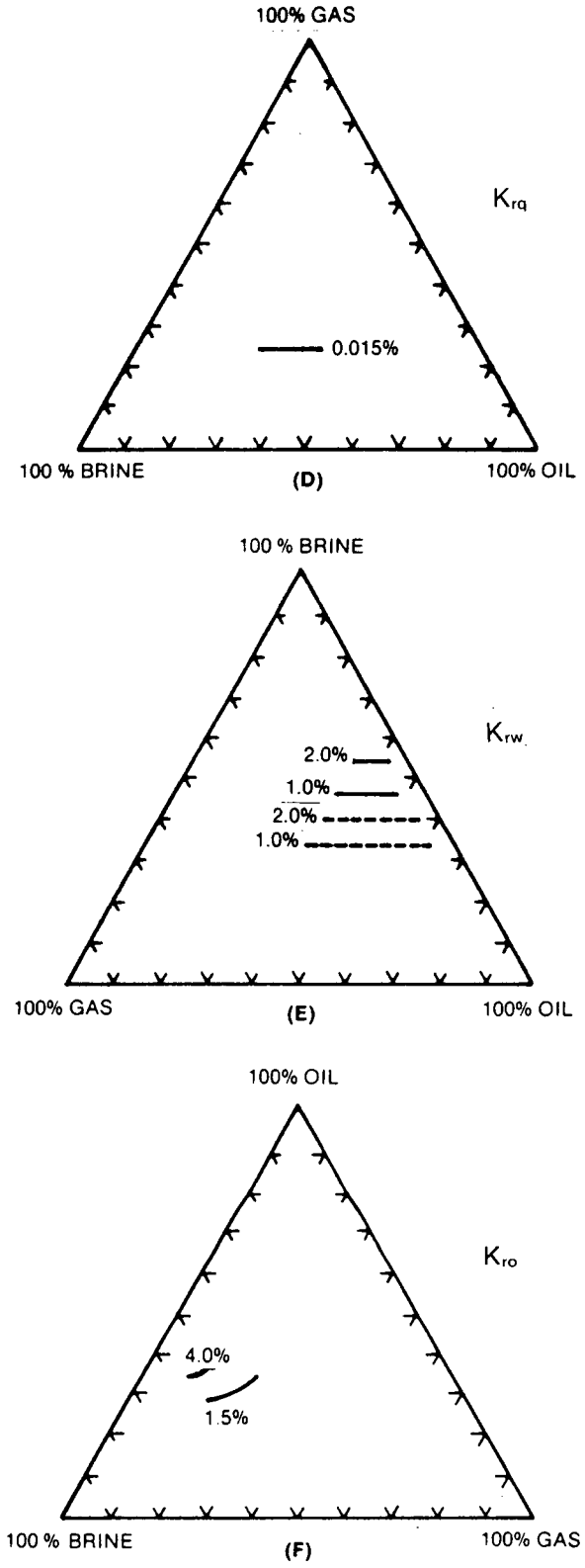

FIGURE 15. - Gas, brine, and oil relative permeability isoperms from 0.97 cP (solid lines) and 10.8 cP (dashed line) brine viscosity tests, core 16.

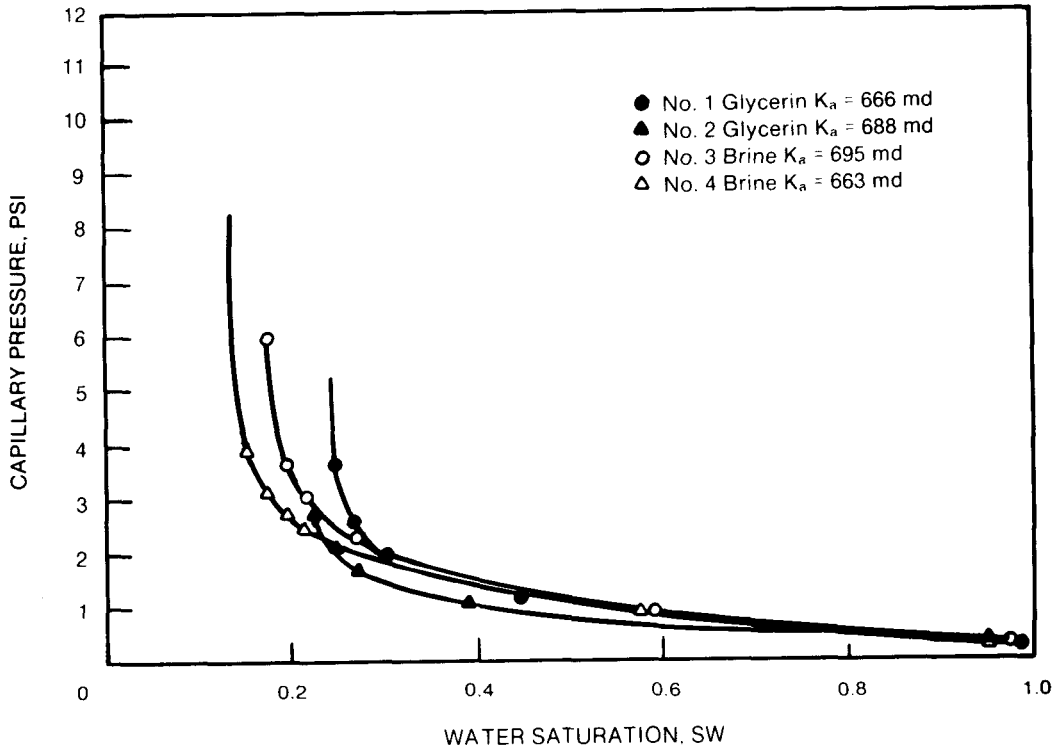

FIGURE 16. - Aqueous-phase and soltrol capillary-pressure curves obtained by centrifuge for various concentration of glycerine/brine mixtures at 75° F.

APPENDIX A

SUMMARY OF LITERATURE REVIEW ON THREE-PHASE RELATIVE PERMEABILITY EXPERIMENTS

Brief Analysis of Published Literature

An outline of published work related to three-phase relative permeability is provided in this appendix. Summary tables have been published by Honarpour et al.[2], Oak et al.[3], and Donaldson and Kayser.[4]

From these summaries, it becomes clear that further studies will be required to delineate the importance of parameters affecting three-phase relative permeability. Therefore, instead of concluding remarks, speculative comments on the difficulties encountered in such studies are provided. Only elaborate and more comprehensive studies with good control on front stability, hysteresis, and wettability will be successful in providing conclusive results.

The most serious problem appears to be the hysteresis effect. Although it is relatively easy to either increase or decrease the saturation of a phase in two-phase systems, it is intrinsically difficult to do so in a three-phase system. In the displacement process, the core is completely saturated with a wetting phase; water, for example, then oil is introduced. When gas is subsequently injected for the determination of unsteady-state, three-phase relative permeability, it causes the oil saturation to decrease. Therefore, oil saturation does not change monotonically; rather, it first increases then decreases. This introduces hysteresis effects which cause relative permeability values to be affected by initial saturations. Several techniques have been tried in which the saturation of oil is held constant, but in those cases, it has not been demonstrated convincingly that relative permeabilities values would be similar as if all three phases were mobile.

A similar problem is encountered during steady-state tests. To cover the entire saturation envelope for three-phase flow on a ternary diagram, the saturation of all three-phases cannot be changed monotonically (because the total saturation cannot exceed 100%) without cleaning or replacing the core. Cleaning has often shown to alter pore and surface characteristics, while samples from the same block have shown to exhibit different flow behavior in many instances. In both instances, considerable data scatter can be expected. To avoid changes, many studies have performed complete tests on the same

sample without cleaning, such that the saturation of two of the phases is monotonic, whereas the saturation of the third phase (usually the wetting phase) is allowed to change direction in small cycles. This procedure has considerable merit provided that it can be ascertained a priori that the third phase is not significantly influenced by hysteresis effects.

A serious limitation in performing three-phase relative permeability tests is time. The equilibration process is quite slow in most instances. To obtain a complete set of data for ternary diagrams, a long time period is required. During long durations, many changes are likely to take place. It appears that many studies have performed tests without allowing enough time for compelete equilibrium. Whether complete equilibrium is important or not for such tests is yet to be determined.

One common problem encountered during these studies was that of drawing isoperms, i.e. the lines of constant relative permeability. All the studies except one have performed experiments without any control on maintaining fixed relative permeability values while changing saturations. For experiments with randomly changing relative permeability values, resulting data were insufficient for drawing well-defined isoperms on ternary diagrams. The situation was further complicated due to data scatter because of operational difficulties previously described. Therefore, curve-fitted ternary diagrams shown in these studies are subjected to individual bias. Some studies have avoided this bias by using multivariate curve-fitting computer routines, but the results are still not unique because of arbitrarily defined constraints.

Oak et al.[3] have recently performed experiments with a fully automated computer-controlled equipment whereby rates are adjusted to determine saturations at fixed values of isoperms. Good control on hysteresis was also possible in this study. Their published results are the only data in which actual data points are shown without curve-fitting. Full automation of three-phase relative permeability equipment seems to be a definite advantage in obtaining accurate data.

The steady-state method is the only technique for three-phase relative permeability determination that does not involve simplifying assumptions for analysis of data. Both unsteady-state and centrifuge methods encounter difficulties in analysis. In the centrifuge method, the relative permeability to gas cannot be determined. In displacement tests, one of the phases has to

be at an immobile condition. The results from both techniques have shown to be influenced by the degree of initial fluid saturation. Grader et al.[20] presented a method of analysis (using self-similar solution) in which all three phases can be mobile concurrently, so that one of the phases does not have to be at residual conditions. Their method, however, has yet to be supported by independent studies on consolidated cores.

TABLE A-1
SUMMARY OF LITERATURE REVIEW ON THREE-PHASE RELATIVE PERMEABILITY EXPERIMENTS

STEADY-STATE

Unconsolidated Sandpacks:

Authors	No. of tests	Fluids	Saturation measurements
Leverett and Lewis (1941)	5 samples, 64 measurements	N_2, Kerosene, +SAE 50 brine	S_o from resistivity, others from material balance
Reid (1956)	98 measurements	air, diesel, brine	S_w by resistivity, Sg by gamma ray adsorption
Snell (1962)[2]	2 samples, 250 measurements	air, diesel + SAE 30 brine	S_w by RCL (radio frequency). Sg by Neutron measurements.
Grader and O'Meara	2 samples, 7 repacking, 5 steady-state and 72 dynamic measurements	water, decane, benzyl alcohol	volumetric, closed loop

Consolidated Cores:

Caudle, et al. (1951)	1 sample, few measurements	air, live oil, connate brine	S_w,S_o by vacuum distillation
Corey, et al. (1956)	9 samples, 62 measurements	gas, polaroid, brine	S_w, S_o, Sg, by gravimetric
Saraf and Fatt (1967)	10 samples/10 measurements	N_2, kerosene, Deuterium oxide	S_w, by extraction, S_o by NMR
Schneider and Owens (1970)	4 samples	N_2, hydrocarbon fractions, brine	S_w by resisitivity, S_g by x-ray
Spronsen (1982)	7 samples	Co_2, 30 cP oil, water glycol (300 cP)	abosrption S_w, S_g, S_o, by gravimetric.
Saraf, et al (1982)	unknown	N_2, Soltrol-130, distilled water	S_w, S_o, S_g by material balance
Guckert (1968)	11 cores/76 measurements	Helium/nitrogen, tagged kerosene (1.9 cP) and brine	S_w by conductivity, S_g by Gamma-Ray absorption
Oak et al (1988)[3]	1 sample, 104 measurements	N_2, tagged 1.772-cP mineral oil, tagged brine	S_o, S_w by dual x-ray absorption

UNSTEADY-STATE

Consolidated Cores:

Authors	No. of tests	Fluids	Saturation measurements
Sarem (1965)	2 samples, 70 measurements	air, brine, Soltrol-130	Vol. measurements of produced-fluids.
Donaldson and Dean (1966)	2 samples, 120 measurements	air, paraffinic oil, distilled water	Vol. measurements of produced-fluids
Schneider and Owens (1970)	4 samples	N_2, hydrocarbon fractions, brine	Vol. measurements of produced-fluids
Saraf, et al. (1982)	unknown	N_2, Soltrol-130, distilled water	Vol. measurements of produced-fluids

[1]Linear means that three-phase relative permeability to a fluid phase depends on its own saturation. Not P.: not presented. Not M.: Not measured.

[2]Snell considered saturation history in analyzing his data, but his tests did not maintain the direction in saturation change to be constant.

[3]Modified after Baker, Thomas SPE/DOE

[4]DOI means saturation change for the three phases is in decreasing, decreasing, and increasing direction.

TABLE A-1 (Continued)
SUMMARY OF LITERATURE REVIEW ON THREE-PHASE RELATIVE PERMEABILITY EXPERIMENTS

Materials	Saturation History	Experimental Method	Isoperms Water	Isoperms Oil	Isoperms Gas
Sandpacks	W-O: Primary dr. W-O-G: Ignored	Steady-state	Linear	Concave	Convex
Sandpacks	W-O: Primary dr. W-O-G: Ignored	Steady-state	Concave	Convex	Concave
Sandpacks	W-O: Primary dr. W-O-G: Ignored	Steady-state	Concave	Convex	Concave
Glass-bead Pack 1" dia x 3' 140-200 mesh	DDI[4]	Both steady-state and dynamic	Concave	Convex (benzyl alcohol)	Convex
Sandstone	W-O: Imbibition W-O-G: IDI	Steady-state	Concave	Concave	Convex
Berea Sandstone	W-O: Primary dr. W-O-G: DDI	Steady-state (Hassler's)	Not M.	Concave	Linear
Boise Sandstone	W-O: Primary dr. W-O-G: DDI	Steady-state	Not M.	Convex	Linear
Nellie Bly Torpedo/ Tensleep, SS Grayburg, LS	W-O-G: DDI, IID	Steady-stage Penn State	Linear	Concave	Concave
Berea Sandstone Weeks Island	W-O:Secondary dr W-O-G: DDI	Steady-state (Centrifuge)	Concave	Concave	Not M.
Berea Sandstone		Steady-state	Linear	Concave	Linear
Torpedo Sandstone	W-O: Primary dr. W-O-G: DDI	Steady-state	Linear	Convex	Concave
Berea Sandstone	W-O) primary O-G) dr. W-G)and imb W-O-G)primary)DDI and)IID	Steady-state (modified Penn State)	Linear Linear	Concave (DDI) Linear (IID)	Concave (DDI) Linear (IID)

Materials	Saturation History	Experimental Method	Isoperms[1] Water	Isoperms[1] Oil	Isoperms[1] Gas
Berea sandstone	W-O: Primary W-O-G: DDI	Unsteady-state	Linear	Linear	Linear
Berea sandstone	W-O: Secondary dr W-O-G: DDI	Unsteady-state	Concave	Concave	Convex
Grayburg Beaverhill Lake	W-O: Secondary W-O-G: DDI	Unsteady-state	Concave	Concave	Concave
Berea sandstone	W-O: Secondary W-O-G: DDI	Unsteady-state	Linear	Concave	Linear

DETAILS

Leverett and Lewis (1941)

Method:	Single core dynamic method (steady state)
Core:	Uncon. sands of different origins, 5-16D, 41-44%.
Fluids:	1.4% NaCl, kerosene + 55% SAE 50 (polar), nitrogen
Mobility ratio:	1.86 to 20.22; isoperms for all phases were found to be independent of the visc. of oil phase.
Packing:	dry-screened sand in a sand cell, vertically upward flow, hand shaking, 80-200 mesh USS,
OBP, BP:[1]	none
Operational:	permit gas, oil and brine simultaneously until equilibrium
Cleaning:	flush with CO_2, then with water
Samples/runs:	5 samples, 64 runs
Typical K_{ro}:	0.01 @ 21%, 0.25 @ 50%, 0.60 @ 72%
End effect:	neglected, but expected to be small due to fairly high Δp
Sat. History:	Hysteresis ignored; W-O: Prim. Dr.
Measurement:	Water by electrical resistivity (conductivity of brine between electrodes), gas by P-V rel.(expansion of gas after closing-in cell [at low pressure brine was injected to boost pressure] near cell-ends through perforated rings).
Calc. proc:	Darcy's law; manual smoothing
Errors:	±6% in dead vol., ±2% for equilibrium; ±1-2% in k_o due to lack of equilibrium, large errors due to dead space and lack of equilibrium possible.
Shape of Isoperms:[2]	Water → Linear, Oil → Concave, Gas → Convex.
Remarks:	Refers to Botset (Trans. AIME 1940, 136, 91) claiming uncon. sands differ from cons. rocks. "Considerable spread of data was encountered in the relative permeabilities to gas and water" --- "Errors due to inaccuracies in measurements were negligible compared to the lack of reproducibility that is characteristic of this type of work." "Isoperms for all phases were found to be independent of the visc. of oil phase" "Visual examination under the microscope shows the presence of an oil film (in some cases containing a very small amount of finely divided water) through which oil flows around each gas bubble. It is not clear whether all gas bubbles are connected. However, the gas bubbles are observed to move jerkily, as opposed to the generally smooth flow of water (and oil when gas bubbles are absent or stationary). This jerky motion of the gas imparts similar motion to at least part of the oil, which

[1] OBP, BP → Overburden pressure, backpressure.
[2] Linear shape of an isoperm implies that it is a function of its own saturation; whereas, both convex and concave imply being function of all three phases.

therefore would be expected to move easier than in the absence of gas at the same oil saturation. Likewise, presence of the oil should act as a partial hindrance to gas flow, both of these conclusions are borne out by the curves of figures 5 and 6."

Snell's Comment: "Leverett and Lewis's results can be interpreted to give oil isoperms convex towards the 100% oil saturation apex (on the usual triangular diagram) over the zone of investigation. It is believed these workers may have given unwarranted emphasis to the two-phase oil/gas and water/oil results from some earlier experiments. The oil/gas isoperms exist only in the line of zero water saturation and cannot be approached in a naturally water-wet system."

Snell's Comment: "Of the 75 oil-phase results given by Leverett and Lewis, it seems that 30 give a poor correlation with their deduced isoperms."

Sarem's Comment: "The oil isoperms reported by Leverett of Lewis also have a tendency to parallel the oil iso-saturation lines at the central saturation region where all three phases flow simultaneously."
"At high oil saturations and low water saturations, the isoperms reported by Leverett and Lewis have a definite curvature."

Caudle, Slobod and Brownscambe (1951)

Method:	Dynamic (Penn State Method, steady-state)
Core:	cons. reservoir sandstone, 25 md; 23%
Fluids:	air, original oil at connate brine sat., polar and live oil.
OBP, BP:	No OBP; seems to have some unknown BP
Operational:	oil sat. was decreased by simultaneous increase of gas and brine
Cleaning:	none
Samples/runs:	One sample;
Typical k_{ro}:	0.025 @ 30%; 0.2 @ 50%; 0.56 @ 72% based on k/k_{rw} @ swc
End Effect:	neglected, thought to be small; flow rates were low to avoid rate effect in gas presence, 2 to 5 days equilibrium time.
Sat. History:	Oil ↓, Brine ↑, Gas ↑ (IDI)*; W-O: Imbibition; noticed hysterisis but ignored the effect
Wettability:	plugs were not 100% water-wet
Measurement:	Weighing and vac. distillation after removing the core at each point.
Calc. proc:	Darcy's law

*IDI,DDI,DD,DI,II,ID, etc. → First letter indicates the direction of sat. change for water, second letter indicates for oil and the third (if present) for gas; D implies drainage, I implies imbibition.

Shape of Isoperms:	Water → Concave, Oil → Concave, Gas → Convex.
Remarks:	Incomplete study, preliminary results. Fig. 8 (p. 148) is good example of sat. gradients

<u>Snell (1961/2) [similar procedure and results by Hosain (1961)]</u>

This study was a continuation of Reid (1956) after removing errors.

Method:	Dynamic (Penn State Method, steady-state)
Core:	Uncons. sand, 7.1D, 35%, highly homogeneous and clean
Fluids:	air, diesel + SAE30, 0.584% Nacl (polar oil) 5 cm/min max for brine and 102 cm/min for gas, much below turbulence.
Mobility Ratio:	8 and 4
Packing:	80-100 mesh BSS silver sand, mechanical shaking, under vacuum in water, 4' OD perspex tube, 4' long, 9 sections, 10 pressure taps.
OBP, BP:	1-4 mm H_2O BP
Cleaning:	None
Samples/runs:	One sample (repacked once), 250 tests.
Typical k_{ro}:	0.075 @ 50%, 0.25 @ 70%
End Effect:	Eliminated by making measurements in a zone away from the ends of the core which showed uniform saturation, the end effect was noticable up to 12 cm from the inlet face and up to 20 cm from the outlet.
Sat. History:	DD, DI, II, ID, evaluated results independently from each other on the basis of sat. history; tests did not maintain the direction in sat. change to be constant (ignored hysteresis); W-O: Prim. Dr.
Wettability:	water-wet, but results suggest a partial change to oil-wet
Measurement:	gas by neutron diffraction (bombardment on a single spot in the middle of the chosen section of the cell). Water by RCL circuit (at radio frequency, thus measuring electrodes conductivity). Pressure in water-phase through alundum barriers in points along cell. Uniform zones of S_w selected
Errors:	±½% at low s_w to 2% at high s_w; ±2% for s_g shown in calib, ±½% error in k_o
Shape of Isoperms:	Water → Concave, Oil → Convex, Gas → Convex.
Remarks:	"Hosain, using the same apparatus as Snell, but using a non-polar oil-phase, has shown that for these oils the behavior is independent of the direction in which saturation change are made. However, where polar oils were used, a distinct differences between drainage and imbibition was noticed." "However, it would not be surprising if the degree of wettability were the controlling factor. Clarification of this aspect will be made if an investigation of three-liquid-phase relative permeabilities can be studied; such studies may become important in miscible/immiscible secondary recovery processes."

"In the present reinterpretation only nine runs showed large discrepancies."
"The DD condition was separate (lower) from ID, II and DI cases, the reason for this difference is not readily apparent but may be due to a partial change from water-wet to oil-wet because of the polar oils used in the earlier work."
"This analysis established that even in homogeneous sandpack, even after prolonged flow at constant rate, considerable saturation variations could occur over the length of the flow cell." Only 10% to 20% in the middle was homogeneous.

Donaldson of Dean's Comment: "Snell's water and oil isoperms were similar to those obtained by Reid, but his gas isoperms were convex toward 100% gas sat."
"Snell demonstrated the dependence of the oil phase on the saturation history."

Reid (1956) (PhD Thesis)

Method:	Single core dynamic (Hassler capillary method, steady-state)
Core:	Uncons. sand, 50-100 D, 38%
Fluids:	air, diesel, 0.58% Nacl (polar oil)
Mobility Ratio:	8
Packing:	25-36 mesh BSS, wet sand, hand tamping
Samples/runs:	98 measurement
Typical K_{ro}:	Unknown
End Effect:	Eliminated by making saturation and pressure measurements away from the ends of the core
Sat. History:	ignored hysteresis; W-O: Prim. Dr.
Measurement:	Water by conductivity between two electrodes, oil by differential absorption of gamma-ray (depends on s_w and s_o). Pressure in water phase through fine sand barriers, from points along cell.
Errors:	±1-2% water, ±5% in gas, errors in k_o not given; electrode corrosion experienced differential. absorption of x-rays possibly caused errors.
Shape of Isoperms:	Water → Concave, Oil → Convex, Gas → Concave.
Remarks:	
Sarem's Comment:	"The curvature of Reid's isoperm is opposite to that reported by Leverett and Lewis" and also previous investigations in general.
Donaldsen & Dean's Comment:	"Reid obtained gas isoperms which were concave towards 100% gas saturation indicating higher permeability to gas in the presence of two liquids."

Corey, Rathjens, Henderson and Wyllie (1956)

Method:	Dynamic (Hassler's capillary method, steady-state)
Core:	Berea sandstone.

Fluids:	$CaCl_2$ brine, polar oil
Operational:	oil was replaced by gas, whereas brine was kept stationary by using semi-permeable membrane. Test cores were saturated with brine prior to oil, brine saturation was constant, one core for one point saturation level.
Cleaning:	each core was used only twice
Samples/runs:	nine samples, 1 test
Typical k_{ro}:	0.01 @ 19%, 0.2 @ 50%, 0.45 @ 75%
End Effect:	minimized due to semi-permeable membranes
Sat. History:	W-O-G: DDI; W-O: Prim. Dr. During oil drainage, oil is replaced by gas; brine is kept constant by using silicine treated semi-permeable membrane. Hysterisis is avoided by using different core samples for each saturation level.
Wettability:	water-wet
Measurement:	gravimetric
Calc proc:	a new method of estimating k_r's is proposed based on ratio of areas in capillary curve. Assumes that brine completely fills smaller pore and wets the larger ones.
Shape of Isoperms:	Water → Unknown, Oil → Concave, Gas → Linear
Remarks:	"gas relative permeability curves obtained on cores with brine present were identical with those obtained on the same core with no brine present." "An increase in oil permeability for a given oil saturation occurs when the water saturation is increased at the expense of gas saturation. This effect is most pronounced in the region of low water saturations." "Thus in a water-wet system, as oil is displaced by water, the oil moves into larger pores at the expense of the gas, as the latter is displaced from the system." "k_{rw} in water-wet and k_{ro} in oil-wet were equal, k_{ro} and k_{rg} with brine were equal to k_{ro} and k_{rg} without brine when plotted against total liquid saturation. However, very small range of saturation does not justify generalizations such as $k_g = f(s_g)$". "Two of the cores had gas relative permeability curves which differed from those of all other cores, particularly in the high liquid saturation regions. Therefore, data from these cores were not used in constructing the gas isoperms." "The scatter in the data through which the gas isoperms are drawn undoubtedly reflects the result of using several different cores to represent one medium." "It has been repeatedly observed that the gas (non-wetting phase) flow behavior is much more sensitive to changes in pore geometry than is the response of wetting phase."
Sarem's Comment:	"This is also supported by Corcy who indicates that, at the region of saturation where all three phases flow, the relative permeability to oil may be assumed to be a function of only oil saturation, at the expense of swell error."

Saraf and Fatt (1967)

Method:	single core dynamic (steady-state)
Core:	Boise sandstone, 1.6D, 26%, 6"L, 1½" Dia.
Fluids:	N_2, kerosene, deuterium oxide
Mobility Ratio:	1.87
Packing:	core in Teflon sleeve
Operational:	brine sat. is kept constant by keeping Δp and q_w constant, the oil sat was lowered in steps by flowing increasing amounts of gas until the oil stopped flowing
Sample/runs:	10 samples, 10 tests
Typical k_{ro}:	.01 @ 32%, .17 @ 50%
End Effect:	eliminated by measuring sat. and pressure 1" away from the ends
Sat. History:	Hysterisis eliminated by using different core samples; no saturation was established twice in the same core; brine constant, oil drainage; W-O-G: DDI, W-O: Primary Drainage.
Wettability:	water-wet
Measurement:	NMR for kerosene sat.; brine by assuming constant and determining by extraction at the end of the test.
Calc Proc:	darcy's law
Errors:	large scatter in data due to the use of different core plugs; k_{rw} and k_{rg} drawn from two-phase data. Δp measured in upper zone only. However, oil sat. was reproducible within 1%, in water within 2%.
Shape of Isoperms:	Water → Linear, Oil → Convex, Gas → Linear.
Remarks:	"Sat. distribution observed along x-axis even after 1 month." "k_r - S is not a unique function of sat. but depends on the sat history even in steady state tests." "To avoid hysterisis effect, no saturation was established twice in the same core. Different cores were used in each run even though a slightly greater scatter in the data had to be accepted because no two cores were identical." "At the max. gas sat attained (40%) the k_{rg} was less than 5%." "Because of this low relative gas permeability, experimental error was high."

Donaldson and Dean (1966)

Method:	Displacement (unsteady-state).
Core:	Berea sandstone, 200 md, 19%, 10.5 cm, 2" = dia; and Arbuckle limestone, 425 md, 11%, 7.8 cm, 2" dia
Fluids:	Soltrol, 0.584% Nacl, air (In the text it says paraffinic hydrocarbon oil, distilled water and air)
Mobility Ratio:	1.1334 cp @ 75° F
Packing:	core mounted in plastic
OBP, BP:	none

Operational:	oil and brine displaced by gas injection only, sat. ranged from 100% water to 100% oil, flow was vertically down at 45° angle
Cleaning:	slowly flowing through the cores a stream of trichloroethane, followed by IPA and water, then dried with air
Samples/runs:	2 samples, 120 readings
Typical k_{ro}:	0.5 @ 50%, 2.5 @ 70%
End Effect:	minimized by using high rates, as high as 0.5 pv/min
Sat. History:	Hysterisis ignored, but looks like W-O-G: DDI and W-O: secondary drainage.
Wettability:	not sure due to cleaning
Measurement:	volumetric measurements of terminal flow rates, terminal saturation calculated by Welges
Calc. Proc:	ext. of Welges two-phase technique to three-phase.
Errors:	expect to be large, large collecting vessels, tilted core
Shape of Isoperms:	Water → Concave, Oil → Concave, Gas → Convex for Berea and Concave for Abruckle Limestone.

Sarem (1966)

Method:	Displacement (unsteady-state)
Core:	Brea-Olinda reservoir core, 257 md, 24%, 7 cm long, 3.2 cm dia, s_{wi} = 61.1%, and Berea outcrop, 275 md, 20%
Fluids:	1.3 cp oil (Soltrol-130), 1.16% Nacl, air
Mobility Ratio:	1.3
Operational:	saturate with one liquid then displace with other immisible liquid at least until b.t, then both liquids are displaced by gas in a standard displacement apparatus
Cleaning:	cleaned, dried, then saturate with one fluid
Samples/runs:	2 samples, 70 readings, 8 tests
Typical k_{ro}:	.002 @ 38%; .026 @ 49%
End Effect:	neglected
Sat. History:	Hysterisis ignored, perhaps all DDI; W-O, Primary Drainage.
Measurement:	volumetric measurements of terminal rates, terminal sat. calculated by Welge's
Calc Proc:	extension of Welge's unsteady-state method to three-phase
Shape of Isoperms:	All linear.
Remarks:	"Assume that the fractional flow of each phase may be taken to be a function of the saturation of only that phase in the limited region of simultaneous flow of all phases (even though in practice this may introduce minor error)" "The saturation history is taken to be invariant in this study." "In accordance with our assumption that the relative permeability of each phase is a function of the saturation of that phase only, the isoperms were drawn as straight lines parallel to the iso-saturation lines." "Note that the initial saturation condition influences both the relative permeability to oil and to water, but only slightly influences the relative permeability to gas" (tested in Berea outcrop only). Lower the initial

water saturation, higher the k_{rw} and lower the k_{ro}; whereas $k_{rg} \neq f(s_{wi})$. "It has been shown that the k_{rs} for three-phase flow, as in two-phase flow, is influenced by initial saturation conditions (similar trend)."

Schneider and Owens (1970)

Method:	dynamic (both Penn State and gas drive)
Core:	Torpedo sandstone, 370 md, 24%
Fluids:	1.7 cp and 26 cp closeout hydrocarbon fraction
OBP, BP:	200 psig back pressure
Samples/runs:	6 sandstones, 2 carbonates
Typical K_{ro}:	0.47 @ 60%, 0.23 @ 50%, 0.006 @ 30%; all at 40% water saturation
Wettability:	both oil-wet and water-wet independent systems,
Measurement:	Gas by x-ray absorption, water by electrical resistivity
End Effects:	Not discussed.
Errors:	Expected to be high due to low Δp
Shape of Isoperms:	Water → Linear, Gas and Oil → not apparent because data is not plotted on ternary diagrams.

Oak, Baker and Thomas (1988)

Method:	Dynamic (Modified penn state, fully automated, steady-state)
Core:	Berea Sandstone, 3" long, 2" dia, fired at 1000 deg. F, 210/160 md
Fluids:	Tagged water (1.06 cP), tagged mineral oil (1.77 cP), and nitrogen (0.0187 cP)
Mobility:	1.67
OBP,BP:	800 psi BP
Operational:	After each meas., either gas rate doubled or water rate halved
Cleaning:	Flushed 20 pv each of 0.5% brine, isopro. alcoh. and pentane. Repeated 2-phase perms. Showed no change in wettability.
Samples/runs:	1 sample, 425 measurements for 2- and 3-phase perms. each, only 104 measurements reported.
Typical Rel. Perm:	DDI: Kro -> 0.05 @ 32%, 0.005 @ 22%, 0.001 @ 20%; Krg -> 0.2 @ 40%, 0.05 @ 20%, 0.01 @ 10%; Krw -> 0.05 @ 62%, 0.008 @ 50%, 0.001 @ 38%; IID: Kro -> 0.009 @ 22%, 0.003 @ 17%, 0.001 @ 11%; Krg -> 0.2 @ 42%, 0.1 @ 39%, 0.001 @ 35%; Krw -> 0.003 @ 49%, 0.0016 @ 42%, 0.0007 @ 41%;
End Effect:	Minimized by placing between two 1-3/4" long, tapered (1-1/2"-7/8") fired Berea, and measuring press. across the test core only.
Sat. History:	Hysteresis minimized by monotonic saturation change; Primary-DDI and IID.
Measurement:	Oil and Water by dual-energy X-Ray absorption
Calc. Proc.:	Darcy's Law
Errors:	Not determined, but seems to be a well-conducted test.
Shape of Isoperms:	For IID: All linear; For DDI: Water -> linear, Gas and Oil -> concave.

Remarks:	Stone's Models: Both Models failed at high Sg, Model I was better than II.

Grader and O'Meara (1988)

Method:	Displacement (unsteady-state)
Core:	Uncons. Glass-beads, 140-200 mesh, 3' long, 1" dia., 4.9-7.8 md, 37% por.
Fluids:	Water (1.14 cP), benzyl alcohol (4.98 cP), decane (0.93 cP non-wetting phase)
Mobility:	4.37
Packing:	Packed in a steel cylinder.
OBP,BP:	None
Cleaning:	No cleaning, repacked for each run
Samples/runs:	16 tests on two packs, Average 12 measurements per test
Typical Rel. Perm:	Kro -> 0.01 @ 42%, 0.05 @ 31%, 0.005 @ 20%; Krg -> 0.1 @ 72%, 0.2 @ 63%, 0.3 @ 45%; Krw -> 0.01 @ 25%, 0.003 @ 17%, 0.0005 @ 10%;
End Effect:	Claimed to be small due to small interfacial tensions involved.
Sat. History:	W-O-G: DDI, W-O: primary drainage
Measurement:	Material balance using fraction collector
Calc. Proc.:	Self-modified Welge-JBN
Errors:	Unknown, expected to be high due to significant data scatter for decane representing gas phase.
Shape of Isoperms:	Water -> concave, Benzyl Alcohol -> convex, Decane -> somewhat convex trend
Remarks:	

Spronsen (1982)

Method:	Centrifuge (Unsteady-state)
Core:	Berea sandstone, 0.5-0.6 um^2, 21%; Weeks Island Reservoir (Friable), 4-5 um^2, 26%; both cores 2" long.
Fluids:	Glycol (35-300-cP), oil (0.91-56-cP), gas
Mobility:	0.02-1.39
OBP,BP:	None
Operational:	After desirable oil and water saturations were achieved by steady-state in core holder, the sample was then centrifuged.
Cleaning:	Cleaned and dried
Samples/runs:	3 tests, 25 measurements, each meas. on a different sample
Typical Rel. Perm:	Berea : Kro -> 0.1 @ 21%, 0.005 @ 25%, 0.0001 @ 15%; Krw -> 0.1 @ 62%, 0.005 @ 42%, 0.00002 @ 21%; Week I.: Kro -> 0.05 @ 30%, 0.005 @ 20%, 0.00001 @ 10%;
End Effect:	Minimized by high rates for 2-phase, then centrifuging for desat.
Sat. History:	W-O-G: DDI, W-O: Secondary drainage.
Measurement:	Initial and final sample saturations determined gravimetrically
Calc. Proc.:	Self-extended centrifuge techique
Errors:	Unknown, but large scatter in the example figure.

Shape of Isoperms:	Water -> concave (Berea), oil -> concave (Both). Krw not measured for Weeks Island. Krg not measured for both.
Remarks:	

Saraf, Batycky, Jackson and Fisher (1982)

Method:	Both Dynamic and Displacement Methods (Steady- and Unsteady-states)
Core:	Berea sandstone, 510-580 md, 23%, 5 cm dia., 20 cm long, fired at 400 deg. C
Fluids:	Distilled Water, refined/filtered mineral oil (soitrol 130) and saturated nitrogen
Typical Flow Rates:	Liquids -> 1.5 meters/day; Gas -> 75 meters/day.
Mobility:	--
Packing:	Self-modified Hassler type core holder
OBP,BP:	1500 psi, 370 psi
Operational:	In displacement tests, uniform saturation of oil and water was first obtained by steady state flow. Flow was then stopped and gas was injected.
Cleaning:	No cleaning, started with evacuation
Samples/runs:	--
Typical Rel. Perm:	Kro -> 0.8 @ 73%, 0.02 @ 50%, 0.001 @ 32%; Krg -> 0.6 @ 53%, 0.1 @ 35%, 0.001 @ 10%; Krw -> 0.3 @ 78%, 0.02 @ 50%, 0.001 @ 37%;
End Effect:	Minimized in steady-state tests by measuring press. gradient in the central 15 cm of the core
Sat. History:	W-O-G: DDI; W-O: Secondary drainage
Measurement:	Volumetric, fluid interfaces were located by scanning a computer-based photometric device.
Calc. Proc.:	By self-written computer program based on Sarem's extension of JBN, used spline-smoothed displacement data in calc.; Darcy's law for steady-state.
Errors:	In saturation is likely because volumetric measurement and central press. gradient
Shape of Isoperms:	Water -> Linear, Oil -> Concave, Gas -> Linear
Remarks:	"Preliminary tests revealed that cleaning with tolune and IPA possibly damaged the core since its permeability to water changed significantly"

Guckert (1968)

Method:	Dynamic (Steady-state)
Core:	Epoxy-coated Torpedo sandstone, 2.21-2.46D, 25%, 2" square, 12" long, dried at 250 deg. F.
Fluids:	0.5% NaCl+ 0.2% NaCO3 Brine, tagged kerosene (1.883 cP) to match absorption with brine, helium/nitrogen
Rate/velocity:	Max. 2.04 cm/min for water, 19.3 cm/min for gas. Reynolds No. much below critical.
OBP,BP:	None
Operational:	Electrical conductivity was obtained by a high impedance volt meter. Brine rates were kept constant.
Cleaning:	None
Samples/runs:	11 cores/76 measurements

Typical Rel. Perm:	Kro -> 0.01 @ 27%, 0.2 @ 48%, 0.35 @ 62%; Krg -> 0.1 @ 42%, 0.02 @ 20%, 0.01 @ 5%; Krw -> 0.4 @ 72%, 0.1 @ 56%, 0.02 @ 38%;
End Effect:	Eliminated by measuring saturation and pressure drops in central section
Sat. History: W-O-G:	DDI; W-O: Primary drainage
Measurement:	Water by electrical conductivity, Gas by Gamma-ray absorption
Calc. Proc.:	Darcy's Law
Errors:	+/- 2% for gas, +/- 1% for water, +/- 3% for oil
Shape of Isoperms:	Water -> Linear, Oil -> Convex, Gas -> Concave
Remarks:	"The paucity of such data (three-phase rel. perm), however, attests to the experimental difficulties encountered in obtaining reliably such data." "Each investigator's calculated values (using theoretical models) agree reasonably well with his own experimental data ---- (however,) it is generally agreed that they are too simplified to predict quantitative relative permeability data". "Inspection of published three-phase gas relative perm.-sat. relations reveals extensive data scatter. Even --- (after) allowances (for errors), the actual positions and shapes of the isoperms presented are questionable". "Repeated usage (in earlier studies) of the same sand for different wetting phase saturations undoubtedly causes a changing wettability condition from run to run. In several instances, the attainment of equilibrium conditions for the large systems used was doubtful". "Application of the relative permeability data obtained in unconsolidated porous media to consolidated porous media may introduce serious error, for various workers have shown that the difference in behavior of the two systems is not simply one of magnitude but also is qualitative in nature". "The use of eleven different cores to represent one medium unquestionably results in data scatter". "Corey et al. have observed that the gas flow behavior is much more sensitive to changes in pore geometry than is the wetting phase". "Most of the points lie below 5% rel. perm. to gas ------ (thus) the percent error was high". "The measurement of relative permeability on a system containing a compressible fluid is complicated by the gas expansion which occurs as the volumetric gas flow rate increases progressively from inlet to outlet due to pressure reduction. As a result of the gas expansion a saturation gradient will exist across the core". "Since the pressure decreases along the length of the core from the inlet to the outlet, gas may go into or come out of solution in various parts of the core ------ (which) may lead to trapping of the gas phase". "For a fixed gas sat., increasing the water sat. at the expense of the oil sat. results in a decrease in the gas permeability. An explanation of this behavior is not readily apparent".

APPENDIX B

NONMETALIC MICROWAVE COREHOLDER TEST

The core sample used during this investigation was a 0.75 x 2 x 4 inch rectangular core jacketed with epoxy resin. The plastic core end pieces added about 2 inches to the overall core length. The Berea sandstone core had a brine permeability of approximately 500 md and porosity of about 22%. Rectanglular core was used for consistency because all previous results based on measurements conducted on rectangular cores.

Figure B-1 is a drawing of the microwave coreholder. The coreholder endcap is machined specifically for 1.5-inch-diameter cores, so the three inlet ports could not be used during this investigation and were plugged. The core end piece welded to the coreholder end cap provided no useful benefit during this experiment and limited the length of the core due to space constraints. Of the four other ports, two were plugged and two were used as inlet and outlet ports to the epoxy core. Tubing of 1/16-inch OD was used to connect the inlet and outlet from the core to the inlet and outlet ports of the coreholder. Long, rectangular strips of microwave absorbing material were taped above and below the core before it was inserted into the coreholder. Valves were placed on the coreholder inlet and outlet lines, and a pressure gauge was placed on the inlet between the valve and core. Valves and a pressure gauge were attached to the two ports on the other end cap to the coreholder. The valves were used to fill and vent the confining fluid, and the pressure gauge was used to monitor the confining pressure.

The fluid used for confining pressure was a silicone liquid commonly used as an electrical transformer oil. The silicone liquid was selected because it has a very low water content and therefore does not absorb much microwave energy. The silicone fluid looks like rock to x-rays, but x-ray absorption by the silicone liquid was not excessive. Samples of epoxy and rubber were immersed in the silicone liquid for several days to test compatibility, and no reactions were noted.

Microwave and x-ray scans were taken of the core and coreholder before and after the coreholder was filled with the confining fluid. The x-ray power settings were 45 kV and 10 mA with window settings of 45/51. The core was subjected to confining pressure in the 1,000 psig range. After vacuum evacuation of the confined core, the core was completely saturated with 1% NaCl brine and scanned as brine was pumped through the core. The core was flooded with 47.8-cP oil to residual brine conditions and scanned. During the oil flood, the core was subjected to injection pressures in the 75 to 100 psig range. Next, the core was flooded with brine to residual oil saturation and scanned. Thereafter, the core was cleaned in situ with pentane and CO_2 and then dried with N_2. Scans were taken of the 'cleaned' core. The core was then vacuum evacuated, and was completely saturated with the 47.8-cP oil by allowing the vacuum to draw the oil into the core. The heavy oil was not sufficiently mobilized by the vacuum, so saturation was achieved by pumping oil into the inlet while pulling a vacuum on the outlet. Additional scans were taken of the core under oil-saturated conditions.

Results

Figures B-2 and B-3 show microwave and x-ray scan results for nine positions within the core under various saturation conditions. These plots are similar to those obtained for other epoxy-jacketed cores that were tested under unconfined conditions. A review of the two figures suggests that the 'cleaned' core was not completely dry; therefore, the 100% oil saturation scan data may have been influenced by the presence of water.

Figure B-4 shows microwave results for four scan positions plotted against x-ray results. The distance between scan positions is approximately 7 mm. The linear trend of the data is a good indication that changes in microwave and x-ray responses were predominantly due to changes in liquid saturations.

Figure B-5 is a two-point (dry and 100% brine saturation) microwave calibration for one scan position, and figure B-6 is a similar two-point (100% brine and 100% oil saturation) x-ray calibration. Using the two-point calibrations, the saturations at S_{or} are 36.9% oil and 69.6% brine for a total saturation of 106.5% rather than 100%. For S_{wc}, the saturations predicted by the two-point calibrations are 72.6% oil and 21.5% brine for a total saturation of 94.1%. Some of the error in scan data is probably due to less-than-complete oil saturation. Additional data analysis techniques, such as compensating for the lack of good 100% oil saturation data by using the relationship between the microwave and x-ray response, as shown in figure 8, can improve the accuracy of the calibrations. This procedure was successfully used to develop accurate calibrations between the x-ray and microwave systems, as described further in this report. However, the primary purpose of this experiment was to determine if accurate saturation data could be obtained using the microwave coreholder, and the answer appears to be yes.

Discussion

During a typical relative permeability experiment using unconfined epoxy-jacketed cores, the possibility of bursting the epoxy jacket or having the epoxy-coating pull apart from the core sample becomes great when injection pressures exceed about 50 psig. The core tested inside the microwave coreholder under a confining pressure of 275 psig was subjected to injection pressures in the 50 to 100 psi range, and no bonding or epoxy failures were noted. As the coreholder is designed to allow confining pressures to 5,000 psig with a 4:1 safety factor, the use of the microwave coreholder and confining pressure will significantly improve experimental flexibility and the longevity of cores tested during three-phase flow tests. Although an experiment using the coreholder may require more time to set up, the time savings may be significant since higher pump rates can be used during the calibration sequence and during relative permeability tests. One significant limitation on the use of rectangular cores at this time is that the end cap is designed for round cores. To alleviate this problem, a new end cap was machined similar to the existing end cap but without the provision for round cores. An investigation is also in progress to find a suitable microwave absorbing material for coating the tie rods to protect the microwave equipment from arcs and to provide a stationary absorber over the check rods.

Summary

1. The microwave coreholder was tested and found to be satisfactory for testing rectangular epoxy-jacketed cores under confining pressure.

2. The use of the microwave coreholder may significantly improve experimental flexibility by allowing cores to be tested under confining pressure. The confining pressure allows higher injection pressures or back pressures to be imposed during flow tests.

3. No significant effects due to the shape of the coreholder were noted in the test data when microwave absorbing material was installed above and below the core in the coreholder, although sufficient space must be left between the metallic surfaces of the coreholder and tubing and the scan interval.

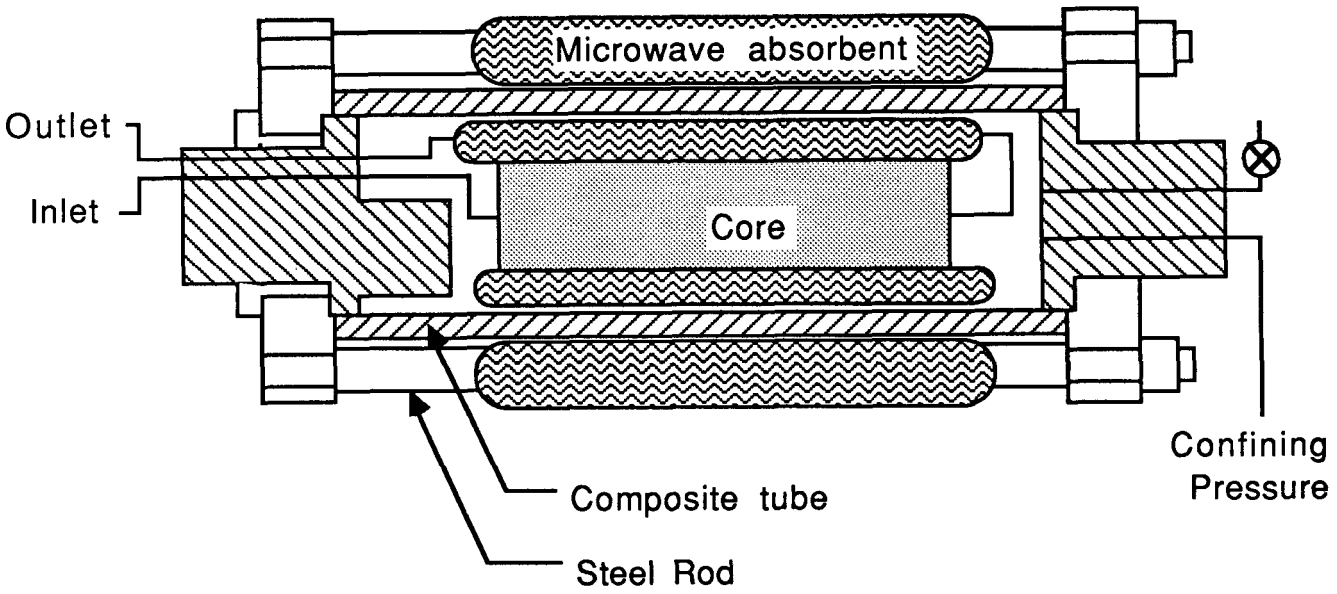

FIGURE B-1. - Schematic of the microwave coreholder.

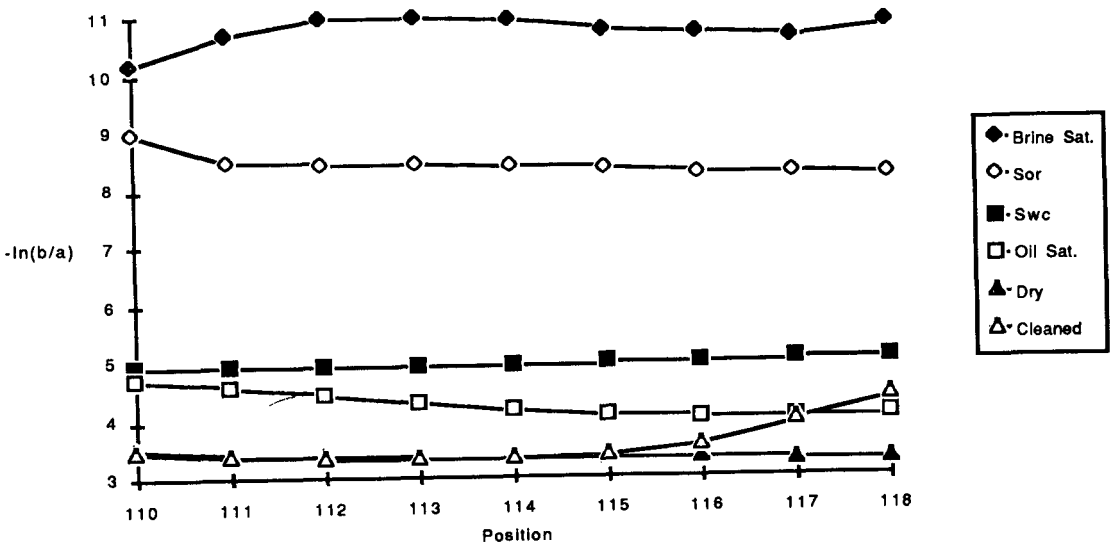

FIGURE B-2. - Microwave results, core 15 in the microwave coreholder.

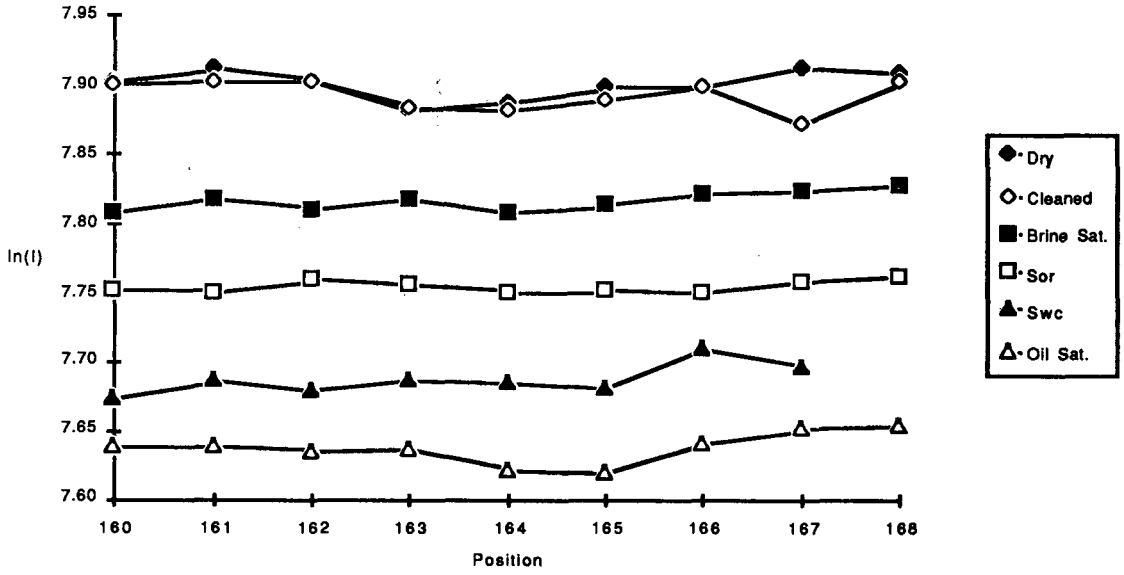

FIGURE B-3. - X-ray results, core 15 in the microwave coreholder.

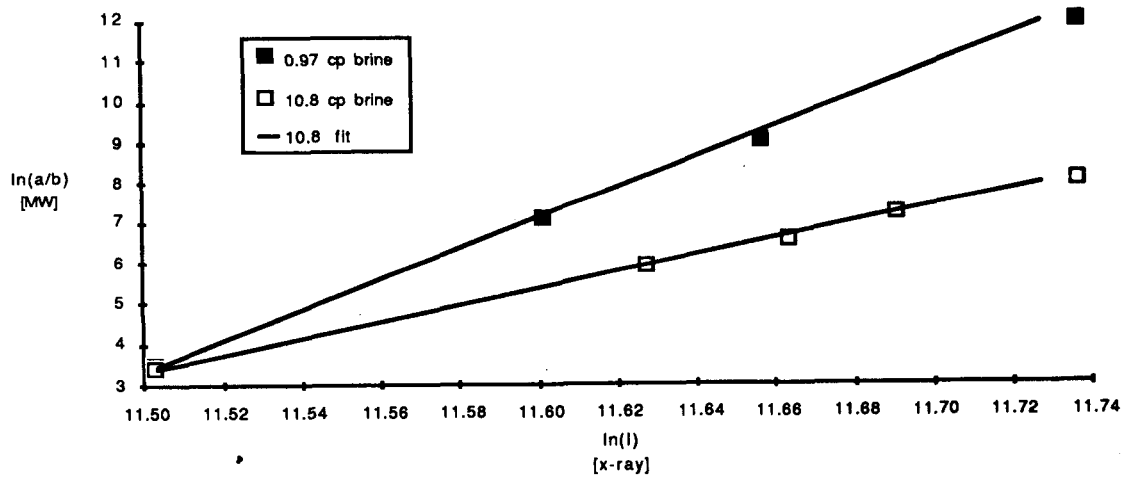

FIGURE B-4. - Comparison of microwave versus x-ray scan results, core 16, position 9.

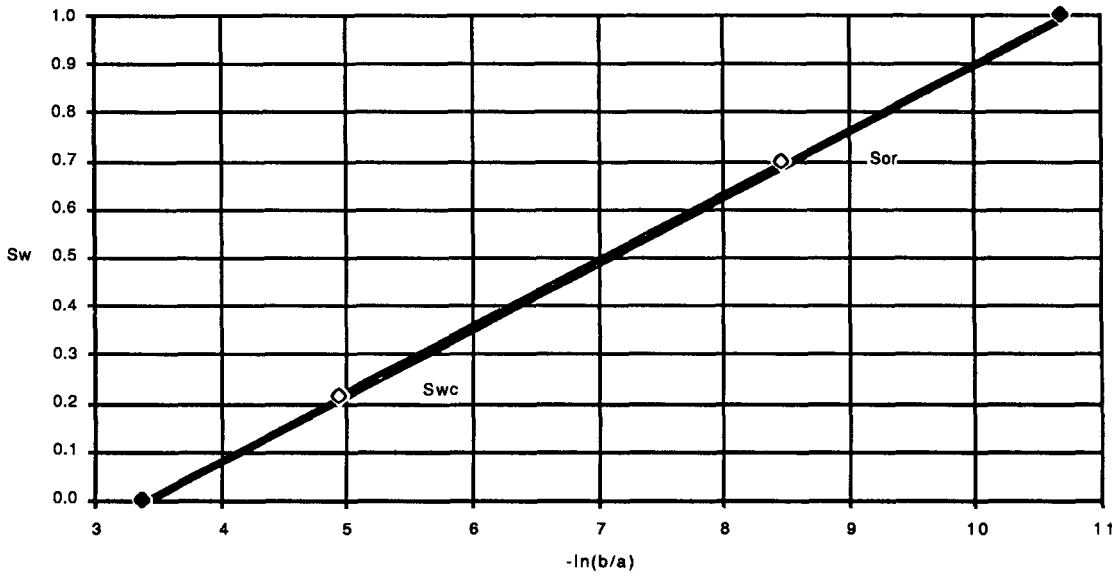

FIGURE B-5. - Two-point microwave calibration for position M111, X161.

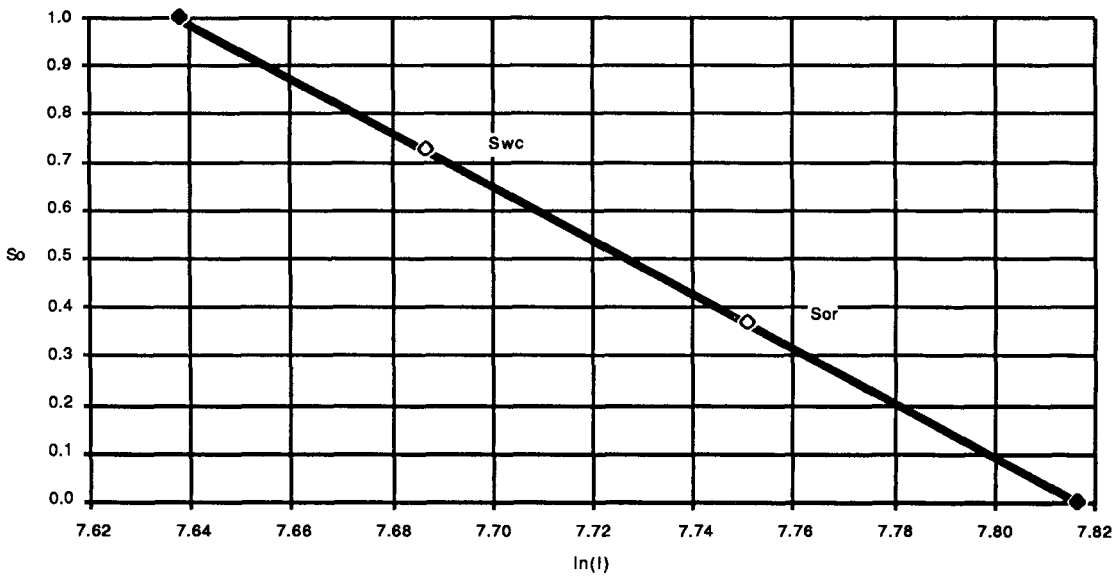

FIGURE B-6. - Two-point X-ray calibration for position M111, X161.

APPENDIX C

CRITERIA FOR MAXIMUM AND MINIMUM RATES AND PRESSURE DROPS

(A) RATES DURING CLEANING AND SATURATION

Maximum Rate: Determine using Reynolds No. to avoid turbulence; a conservative stable rate criterion to avoid viscous finger, and the experienced-based criterion to avoid fine migration. Select the lowest of the three criterion as the maximum allowable rate.

$$W \leq \frac{6.33\ (10^{10})\ \mu\ A\ (0.1)}{\beta\ k} \quad \text{(Eq. 2-16 i Katz' Handbook)}$$

where β = turbulence factor, ft^{-1} = f (k, ϕ) (Use Katz' Handbook)
W = mass flow rate, lb_m/sec (1 lb_m = 453.59 grams)
k = permeability, md
μ = viscosity, cP
A = cross-sectional area of flow, ft^2 (1 ft = 30.48 cm)

Typical values: $\beta \cong 10^7\ ft^{-1}$ for a 400 md or higher permeability) sand of 20% or higher porosity

$$\upsilon_{N_2} = 13.532\ ft^3/lb_m \text{ @ } 60°\text{ F and 1 atm.}$$

$$\mu_{N_2} = 0.017884 \text{ cp @ } 300°\text{ K (i.e. room temp.)}$$

$$\upsilon_s = \frac{0.0853\ k\ (\rho_B - \rho_A)}{\mu_B[(\frac{\mu_B}{\mu_A})^{1/4} - 1]} \quad \text{(Blackwell correlation)}$$

where k = permeability, md
ρ_B = density of displacing fluid, lb_m/ft^3
ρ_A = density of displaced fluid, lb_m/ft^3
μ_B = viscosity of displacing fluid, cP
μ_A = viscosity of displaced fluid, cP

The maximum rate to avoid fine migration is sometimes found during the experiment in form of sharp injectivity changes. If this happens, the core has already been damaged. Start with a new core and do not exceed 75% of the rate at which failure took place.

Minimum Rates:

Use one of the following capillary No. criterion to minimize capillary end effects:

$$N_c = \frac{q\mu}{A\ \sigma\phi} \frac{(cm^3/sec)(cP)}{(cm^2)(dynes/cm)(frac)} \geq 10^{-4} \quad \text{(Melrose and Brandner)}$$

$$\text{or} \quad N_c = \frac{k}{\phi}\frac{\Delta P}{L\sigma} = \frac{(md)(psi)}{(frac)(ft)(dynes/cm)} \geq 5 \quad \text{(Taber, 1984) [1 ft = 30.48 cm]}$$

If σ is not known, assume 35 dynes/cm between oil and water, but consult a handbook first. Typically, 1 ft/d is a minimum rate. However, the flow behavior changes when the fluids have interfacial tensions lower than 0.1 dynes/cm, in which case 2.5 ft/d may be a typical minimum rate.

Maximum Pressure: Do not exceed 75% of the safe test pressure without structural damage to avoid failure of the epoxy during the test.

Minimum Pressure: Operate well above the atmospheric pressure. For pressures approaching atmospheric, correct for Klinkenberg Effect (slip) as described in Katz' Handbook (Figs. 2-14 and 2-15).

As a first approximation for N_2, use:

$b = 6.9\ k_L^{-0.36}$ (Jones, S. C., SPEJ, Oct. 72, p. 383)
where b is in psi and k_L is in md.

(B) RATES DURING THE TEST

Maintain the rate during the test according to Rapoport and Leas' linear scaling criterion:

$$\left.\frac{\sigma\,(\cos\phi)}{L\upsilon\mu}\right|_{core} \geq 5\ \left.\frac{\sigma\,(\cos\phi)}{L\ \upsilon\mu}\right|_{reservoir} \quad \text{OR} \quad \left.\frac{k\ P_T}{L\ \upsilon\mu}\right|_{core} \geq 5\ \left.\frac{k\ P_T}{L\ \upsilon\mu}\right|_{reservoir}$$

where L = length
υ = frontal velocity
μ = viscosity of oil
σ = IFT between oil and brine
ϕ = contact angle
k = absolute permeability
P_T = threshold pressure

If field frontal velocity is not known, assume 1 ft/d, determine P_T experimentally. Use any set of units in above inequalities, as long as units are same in both the core and the reservoir.

☆U.S. GOVERNMENT PRINTING OFFICE: 1989-661-023/00011